Deciphering the many maps of the Xingu – an assessment of deforestation from land cover classifications at multiple scales

Kalacska M[1], Arroyo-Mora J.P[2], Lucanus O[1], Sousa L[3], Pereira T[4], Vieira T[4]

[1]Applied Remote Sensing Lab, Department of Geography, McGill University, Montreal QC, H3A 0B9 Canada

[2]Flight Research Lab, National Research Council of Canada, Ottawa ON, K1V 2B1 Canada

[3]Laboratório de Ictiologia de Altamira, Universidade Federal do Pará, Altamira PA 68372040, Brazil

[4]Universidade Federal do Pará, Altamira PA 68372040, Brazil

Abstract

Remote sensing is an invaluable tool to objectively illustrate the rapid decline in habitat extents worldwide. Over the years, diverse Earth Observation platforms have been used to generate land cover maps, each with its unique characteristics. In addition, considerable semantic differences between the definition of land cover classes results in inevitable differences in baseline estimates for each class (e.g. forest). Here we compare forest cover and surface water estimates over four time periods spanning three decades for the Xingu River basin, Brazil, from pre-existing remotely sensed classifications for this area based on both optical and radar data. Because forest health in this area is directly related with the health of the freshwater ecosystem, we illustrate potential impacts of map choice on conservation of fish fauna. Understanding differences between the many remotely sensed baselines is fundamentally important to avoid information misuse and objectively decide on the most appropriate dataset for each conservation or policy making question. Our findings demonstrate the importance of transparency in the generation of remotely sensed datasets and in the importance of users familiarizing themselves with the characteristics and limitations of each data set chosen.

Keywords: satellite image, radar, Landsat, forest, biodiversity, MODIS, ALOS/PALSAR, TanDEM X

Introduction

Earth observation from satellite imagery is fundamentally important for conservation (Li et al. 2016; Rose et al. 2015). Since the early days of deforestation mapping from satellites (Skole and Tucker 1993; Townshend and Justice 1988; Westman et al. 1989), remote sensing has become an invaluable tool (O'Connor et al. 2015; Paganini et al. 2016; Proenca et al. 2017) for objectively illustrating the rapid decline in habitat extent (Pimm et al. 2001). *Land-Use* and *Land-Cover Change* (LUCC) due to agricultural expansion, hydropower development and pastureland intensification are among the most visible footprints of anthropogenic influence on the landscape (Foley et al. 2011; Rockstrom et al. 2009). A growing world population, increasing consumption and global food security concerns have led to surges in production of agricultural and animal products (Dias et al. 2016; Godfray et al. 2010; Lambin and Meyfroidt 2011) that cause acute LUCC transformations in the tropics (Hansen et al. 2010).

Amazonian forests are both home to nearly a quarter of the world's known terrestrial biodiversity and are drivers of global atmospheric circulation (Malhi et al. 2008). As such, they are vital not only for biodiversity conservation but also for climate change mitigation (Pereira and Viola 2019). Humans have modified this biome since pre-Columbian occupation (Levis et al. 2017; Lombardo et al. 2013; McMichael et al. 2017). Although Amazonian deforestation rates have slowed in the early 2000s (Nepstad et al. 2014), Brazil's recent policies have progressively favored the energy production and agri-business sectors, weakening environmental laws (Brancalion et al. 2016; Fearnside 2016a; Rajao and Georgiadou 2014). Across the Amazon, the construction of roads that enable transport of timber (legal and illegal),

deforestation for cattle ranching and the establishment of large monocultures (e.g. soy, corn, cotton) are the leading causes of Amazonian deforestation and deterioration of soil and water quality (Abell et al. 2011; Dias et al. 2015; Durigan et al. 2013; Ferreira Marmontel et al. 2018; Gauthier et al. 2019; Ilha et al. 2019; Klarenberg et al. 2019; Lees et al. 2016; Lessa et al. 2015; Macedo et al. 2013; Mello et al. 2018a; Mello et al. 2018b; Rodrigues et al. 2018; Zimbres et al. 2018). In soybeans alone, Brazil increased its gross production by 94% between 1991 and 2013 (FAO 2016). The Brazilian Ministry of Agriculture estimated that grain and beef production will increase by nearly 30% by 2020 (MAPA 2015). Policies favoring agribusinesses have also deregulated the use of agrochemical products, many of which have been banned in other countries for years; 30% of agrochemical products used in Brazil are prohibited by the European Union (Costa et al. 2018). The widespread use of these agrochemicals has considerably increased the contamination indexes of soil and water bodies across the country. Furthermore, a resurgence of deforestation is expected in the near future as the current government is decreasing conservation policies throughout Brazil (Fernandes et al. 2017; Freitas et al. 2018; Scarrow 2019; Tollefson 2018).

The Xingu River, traversing ~2,700 km through the States of Mato Grosso and Pará, is the fourth largest tributary of the Amazon River. Its basin covers 51 million hectares, of which 20 million hectares are Indigenous land and 8 million hectares are protected land (Villas-Boas 2012). The Xingu watershed encompasses a complex geomorphological base (Sawakuchi et al. 2015; Silva et al. 2015) which promotes an extraordinary aquatic biodiversity and high rates of endemism (Sabaj Perez 2015). There are an estimated 600 species of fish, 10% of them endemic to the river basin (Barbosa et al. 2015; Camargo et al. 2004; Chamon and Sousa 2017; Cramer

and de Sousa 2016; Fitzgerald et al. 2018; Giarrizzo et al. 2015; Sousa et al. 2018; Varella and Ito 2018).

Cattle have been present on the Xingu floodplains for over 100 years, but prior to the 1970s the herds were relatively small, and deforestation was minimal (Goulding et al. 2003). In the 1980s, large herds were introduced. As a result, the natural forest outside of protected areas and Indigenous lands in an area larger than France has been either deforested or heavily modified (Dias et al. 2016; Goulding et al. 2003). The displacement of the cattle ranches by large-scale agriculture subsequently led to the greatest rates of deforestation in the region (Barona et al. 2010). Proliferation of genetically modified soy has further increased crop yields; the basin provides 8% of the World's soy production. Mega scale soy plantations are considered as one of the main threats to the environment and rural livelihoods in Brazil (Fearnside 2001).

The Xingu basin also has an intricate mosaic of Indigenous tribes and "ribeirinhos" living on the floodplain; continuous human occupation has modified the landscape over at least the last 1500 years (Schwartzman et al. 2013). Today, twenty-five groups/tribes of Indigenous peoples are recognized, the most well-known being the Juruna, the Araweté and the Kayapó. In addition, over 200 ribeirinhos settlements of various sizes from single family occupations to small communities are estimated to reside on the floodplains of the river (Schwartzman et al. 2013).

While conservation priorities often neglect ichthyofauna (Abell et al. 2011; Nogueira et al. 2010; Stiassny 1996), some initiatives have begun to include freshwater ecosystems, recognizing the divergence of aquatic and terrestrial diversity (Abell et al. 2008; Beaumont et al. 2011; Dinerstein et al. 2019; Olson and Dinerstein 2002). Quantifying change in a biologically and anthropogenically diverse landscape such as the Xingu basin is paramount. Given its large extent, remote sensing derived land cover products are the most efficient sources of such

information. Importantly, these data also provide historical assessments of change for the last four decades. Several land cover products have been produced by different agencies/groups, at varying scales and time periods. Despite individually reporting high levels of accuracy, uncertainty and disagreement between them is well known (Foody 2004; Foody 2006; Fritz and See 2008; Herold et al. 2006) including limited agreement on the spatial distribution of the individual classes (McCallum et al. 2006; Tsendbazar et al. 2016). Therefore, despite acknowledgement of deforestation as a primary driver of biodiversity loss, uncertainty in baseline estimates persists (Sexton et al. 2016). Our objective is to compare forest cover and surface water estimates over time for the Xingu basin from pre-existing remotely sensed classifications in order to determine potential impacts of land cover map choice on conservation of fish fauna. We also include a newly developed publicly available classification for the region using Landsat data (Kalacska et al. 2019). Forest health in this area is directly influences the health of the fresh water ecosystem. Therefore, changes in forest cover and fragmentation have a negative impact on the aquatic species, many of them endemic to the region. Given the current political will in Brazil towards conservation in an ever-changing international economic climate (Abessa et al. 2019; Escobar 2019; Fuchs et al. 2019), understanding differences between the many remotely sensed baselines is fundamentally important to avoid information misuse and objectively indicate potential issues when used for conservation or policy making.

Materials and Methods

STUDY AREA

The study area is ~1.3M km^2 encompassing the Xingu river basin, Brazil (Figure 1). This area includes portions of five states (Amazonas, Pará, Mato Grosso, Tocantins and Goiás) and

two diverse biomes (Amazonia and Cerrado). The Upper Xingu headwaters are spread across a sedimentary basin (Parecis basin) (Sabaj Perez 2015). Many of these headwaters have little or no protection and are increasingly affected by industrial agriculture, leading to massive erosion of the riverbanks as well as contamination from pesticides and fertilizers (Sanches et al. 2012). Recent human activity has increased industrial agriculture (i.e. soy, cotton and corn) and extensive cattle farms leading to deforestation and associated decrease in stream water quality (Barona et al. 2010; Durigan et al. 2013; Mello et al. 2018b; Stella and Bendix 2019). A more reliable road system has also opened not only the agrarian frontier (Schmink et al. 2019) but has also facilitated artisanal illicit gold mining operations leading to elevated mercury contamination (Da Silva et al. 2018a). These headwaters are home to a number of endemic fishes (e.g. the small cichlid *Apistogramma kullanderi,* catfish *Hartia rondoni* and characins *Moenkhausia petymbuaba, M. chlorophtalma* and *Knodus nuptiales*) with distributions limited to one or few of the rivers/streams.

The ichthyofauna of the middle portion of the river that is draining Pre-Cambrian rocks of the Brazilian Shield, spanning from Sao Felix do Xingu to upstream of Belo Monte north of the Volta Grande, differs greatly from the headwaters. The rapids of the middle Xingu, where most of the fish diversity and endemism is found (e.g. 20 endemic loricariid catfish such as *Hypancistrus zebra*, *Pseudacanthicus pirara* and *Scobinancistrus aureatus*), are being destroyed by hydropower development. The Belo Monte dam complex, the third largest in the world, operates on a run-of-river basis with electricity generation varying according to the river inflow. Its reservoir flooded an area of 516 km^2 (Lessa et al. 2015). This follows an unfortunate trend of other tropical rivers around the globe (Fearnside 2016a; Latrubesse et al. 2017; Lees et al. 2016; Winemiller et al. 2016). The highly specialized species of fishes and other aquatic organisms

adapted to rheophilic habitats are not able to survive in the new conditions (Lujan and Conway 2015). Also, almost all species rely on the flood pulse of the river, the alternation between a high water level during the rainy season and low water level in the dry season, to complete their life cycle (Junk et al. 1989). For the Xingu, the natural flood pulse was on average 4.8 m (Barbosa et al. 2015). The artificial regulation of the water level without mimicking the natural pulse has already begun to have devastating effects on the ichthyofauna (Souza-Cruz-Buenaga et al. 2019). In addition, in the section of the Volta Grande dewatered by the Belo Monte Dam, there is yet another project, called "Projeto Volta Grande" planned by the Belo Sun mining company, to begin massive gold extraction in an already weakened ecosystem (Tófoli et al. 2017).

The lower portion where the Xingu enters the lowland of the Amazonas sedimentary basin is home to another fish fauna comprised of both Volta Grande species, and those commonly seen in much of the Amazon lowland (e.g. *Phractocephalus hemioliopterus* the redtail catfish and *Brachyplatystoma filamentosum* the piraiba). Endemics of this portion of the river include *Hypancistrus* sp. “acari pão” and the recently described *Panaqolus tankei*.

DATA

We downloaded ten freely available regional, country-wide and global land cover and surface water classifications created from remotely sensed data (Table 1). We chose four time periods for which multiple datasets were available: 1989-1992, 2000, 2010, 2014-2018. Because each dataset was created from different imagery, with varying methodologies and have different output characteristics (e.g. spatial resolution, definition of forest) we evaluate each dataset in context to illustrate their similarities and differences. The spatial resolutions vary from 25 m

(JAXA Global Forest / Non-forest, Shimada et al. (2014)) to 300 m (ESA Land Cover CCI, Defourny et al. (2016)) and include both optical and radar satellite sensors (Table 1).

From the optical satellite data, the Terra MODIS Vegetation Continuous Fields (VCF) (Dimiceli et al. 2015) and Global Forest Change (Hansen et al. 2013) classifications provide pixels values of percent tree cover at 250 m and 30 m spatial resolutions respectively. For both, we applied a threshold of ≥ 30% to be consistent with the Brazilian forest definition (Gilbert 2009). Generated yearly, the Terra MODIS VCF product is a sub-pixel-level estimation of surface vegetation cover. It is produced from monthly composites of Terra MODIS 250- and 500-meter resolution reflectance imagery and land surface temperature (Dimiceli et al. 2015). The Global Forest Cover baseline map (Hansen et al. 2013) was generated from cloud free mosaics of growing season Landsat 7 ETM+ images for the year 2000. Training data were generated from high spatial resolution Quickbird satellite imagery, as well as pre-existing vegetation continuous field maps derived from Landsat and MODIS imagery (Hansen et al. 2003; Hansen et al. 2011).

The ESA CCI Land Cover product (300 m spatial resolution) was generated for three reference periods each spanning five years to minimize cloud cover (Bontemps et al. 2013). The primary data sources for these classifications are MERIS Full Resolution (FR) images supplemented with MERIS Reduced Resolution (RR) and SPOT-VGT imagery. Consistency with reference datasets such as GlobCover (Arino et al. 2008) and GLC2000 (European Commission 2003) was verified in the preparation of the land cover maps. Validation was performed at an observational unit of 81 ha with samples derived from Google Earth, Landsat TM or ETM+ imagery and multi-temporal SPOT-VG indices.

The Fish + Forest classifications were created from cloud free mosaics of Landsat TM5 and Landsat 8 OLI imagery (Kalacska et al. 2019a). Due to the seasonal extensive cloud cover in the region each mosaic represented the median cloud free reflectance over a reference period of 2-5 years. Covering the smallest overall area of all the datasets examined, training data were generated based on field visits throughout the study area. No other pre-existing datasets were used in the classification process.

PRODES is a yearly product for the Amazon to monitor clear-cutting. It is one of eight forest monitoring systems developed by the Brazilian government (INPE 2015; Rajao and Georgiadou 2014; Rajão et al. 2017). TerraClass utilizes deforestation vector data from PRODES supplemented with satellite imagery from Landsat and MODIS (validated by SPOT-5 imagery) to monitor LUCC in the Brazilian Legal Amazon (de Almeida et al. 2016). MapBiomas classifications are yearly land cover products generated from Landsat imagery (MapBiomas Project). The products are developed separately by biome; here we include subsets for the Amazon and Cerrado. For the MapBiomas data, model training and validation samples are generated from reference maps including TerraClass, PRODES, Global Forest Cover, ESA CCI and others.

The TanDEM-X global forest classification (50 m spatial resolution) was generated from bistatic interferometric synthetic aperture radar (InSAR) data (HH polarization, X-band) acquired over the 2011-2015 period for the generation of a global digital elevation model (Esch et al. 2017; Martone et al. 2018). Forest is defined as > 60% tree cover from the Global Forest Change map (Hansen et al. 2013). The JAXA global forest classification (25 m spatial resolution) is a yearly product (Shimada et al. 2014) generated from HH and HV polarized L-

band Synthetic Aperture Radar (PALSAR and PALSAR-2). To be consistent with the FAO definition, areas with a tree cover ≥ 10% are included in the JAXA global forest dataset.

While the surface water class was included in eight of the landcover classifications described above, we also examine the EC JRC/Google (Pekel et al. 2016) product created exclusively for surface water (1984 – 2015 period). We include the percent occurrence and maximum extent layers. To create a binary water/terrestrial classification we applied a threshold of 30% to the occurrence layer. Lastly, the HydroSHEDS river network is a model of the world's rivers derived from the SRTM GL3 digital elevation model (DEM). The network has been hydrologically conditioned using a sequence of automated procedures including sink filling, stream burning, and manual corrections, among others (Lehner et al. 2008). This dataset is different from the others because water occurrence is not directly observed, it is derived from a hydrologically conditioned DEM.

Each dataset was subset to the ~1.3M km^2 area of interest (Figure 1) and total forest and water (where available) areas were calculated. A fragmentation analysis focused on four main class metrics of forest cover and their change over time for the different land cover classifications with FragStats v4 (McGarigal et al. 2012). Class area (CA) and percentage of landscape (PLAND) are important measures of landscape composition; specifically, how much of the landscape is comprised of a particular land cover (McGarigal et al. 2012). In this study, CA is a good indicator of the total forest area lost over time, while PLAND allows for comparison between maps of the percent of forest lost over time. For the three classifications available for all four time periods (i.e. ESA, Fish + Forest and MapBiomas), two additional indices were calculated: Largest Patch Index (LPI) and the Landscape Division Index (DIVISION). LPI measures the change in the landscape comprised by the largest patch, while

DIVISION is a standardized measure of the probability of two randomly selected pixels in the landscape not being located in the same patch of the corresponding patch type (McGarigal et al. 2012). DIVISION ranges 0 - 1, with a value of 0 when the landscape is comprised of a single patch. Due to a software limitation (32-bit software) the 25 m and 30 m spatial resolution datasets were resampled to 90 m prior to the calculation of these fragmentation metrics.

Spatial fragmentation analyses consisting of Entropy and Foreground Area Density (FAD) were calculated for each dataset with the GUIDOS Toolbox (Vogt and Riitters 2017). Spatial entropy is the degree of disorder in the spatial arrangement of the forest class. A single compact forest patch has minimum entropy whereas maximum entropy is found when the forest class is split into the maximum number of patches given the area and dispersed equally over the entire area (i.e. checkerboard pattern) (Vogt and Riitters 2017). FAD measures the proportion of forest pixels at five observation scales (7, 13, 27, 81, 243 pixels). Results are classified into six classes: < 10% (rare), 10-39% (patchy), 40-59% (transitional), 60-89% (dominant), 90-99% (interior), 100% (intact). The final maps represent the average from the five observation scales (Vogt and Riitters 2017). Morphological Spatial Pattern Analysis (MSPA) (Soille and Vogt 2009) was applied to each forest classification to map morphometric details of the forest patches. Seven mutually exclusive classes of core, islet, loop, bridge, perforation, edge, and branch were mapped by MSPA for forest in each dataset.

Results

The forest cover maps for the four time periods are illustrated in Figure 2. Overall, the trend across datasets is a loss in forest area over time as expected. Differences among the maps can be attributed to several factors including spatial resolution, cloud cover, input data, data quality, methodology, etc. For example, the forest NE of Vitoria do Xingu is noticeably absent in

the PRODES 2010 map likely due to cloud cover. Also, the two coarse datasets (ESA and MODIS) have a more generalized representation of the forest cover. In addition, even within time periods there is a both an area and spatial arrangement difference in forest cover between datasets (Figures 1 and 2). For the earliest time period the region south and east of Canarana as well as north of Santarém have greater forest cover in the MapBiomas map than in either ESA or Fish + Forest (Figure 1a). The same pattern can be seen for the other three time periods as well with the MapBiomas data showing the greatest forest cover in that region. For the 2000 time period the Global Forest Cover map is most similar to MapBiomas showing greater forest cover in the southern and eastern sections than the other classifications (Figure 1b).

At such a large scale (Figure 1), most of the datasets appear similar and as such it may be difficult for users to choose between them. However, the forest class statistics reveal differences in the total area classified as forest (CA) (Figure 2). For example, for the year 2000, the difference between the minimum (67% Fish + Forest) and the maximum (76.2% Global Forest Cover and MapBiomas) is just over 120,000 km^2, approximately the area of Pennsylvania. For the most recent time period that difference increases to just over 220,000 km^2 (approximately the area of Utah) between PRODES (52.5%) and MapBiomas (69.3%). It is important to note that the portion of the State of Goías in the study area (3% of total area) is not included in the PRODES estimates. The deforestation trend between datasets is largely consistent (Figure 2); there is a decrease in forest area over the four time periods. While all datasets continue to show a decrease in forest area between the 2010 and the most recent period (2014-2018), the MapBiomas and PRODES datasets indicate a slight increase. For PRODES the reason is likely due to cloud cover contamination in the 2010 data (also seen in Figure 2c) leading to a lower

overall area of forest. The JAXA data indicate the greatest forest loss between those two time periods.

The PLAND trends are consistent with CA, with forest loss ranging from 10.3% between 1992-2015 for ESA, to 15.6% and 15.1% for Fish + Forest and MapBiomas, respectively. There is also an overall decrease in the area of the largest patch (LPI) over the four time periods for ESA and Fish + Forest (Figure 3c) consistent with temporal erosion of the main core of the intact forest (Figure 4a). In contrast, the LPI indicates a recovery of the largest patch area from 2010 to 2017 from MapBiomas (Figure 3c). Furthermore, DIVISION shows that a consistent fragmentation process is occurring in this area over the four time periods based on the ESA and Fish + Forest classifications (Figure 3d). As with the LPI metric from MapBiomas, DIVISION also indicates a decrease in fragmentation between 2010 and 2017 for this dataset (Figure 3d).

Temporal visualization of deforestation (Figure 4a) illustrates a gradual reduction of the forest cover with the deforestation encroaching upon the core forest areas. While substantial deforestation occurs in Mato Grosso, in Pará the effect of roads (e.g. north of Castelo do Sonhos and between Itaituba and Altamira) leading to increased deforestation is evident. Marked deforestation for urban growth and increased agricultural development around Sao Felix do Xingu can be seen between 1989 and 2000 with forest loss in the sustainable use area (Figure 4b) west of the town. The majority of the remaining intact forest in both Pará and Mato Grosso is within the boundaries of protected areas and Indigenous territories. Heavy deforestation is also seen in the Volta Grande and around Altamira after 2010 attributable to the construction of the Belo Monte dam (Da Silva et al. 2018b) (Figure 1, Figure 4a).

The spatial FAD (Figure 5) and entropy (Figure 6) results illustrate large differences in the landscape (i.e. fragmentation, connectivity and intact forest) depending on the choice of

forest cover map. For the oldest time period (Figure 5a) the most noticeable difference is the lack of intact forest west of Querencia from the ESA data. Due to the coarser spatial resolution of the ESA data (300 m vs 30 m for MapBiomas and Fish + Forest) the areas of forest in Mato Grosso at this time are not large enough to be considered 'intact' based on the multiple scales of assessment in the FAD metric (i.e. the largest scale of FAD is 243 pixels which results in a moving window of 72.9 x 72.9 km for ESA). There is less intact forest around Sao Félix do Xingu based on the Fish + Forest dataset due to the increased number of small deforestation patches which are not present in the MapBiomas data. Similar trends can be seen in subsequent time periods with the coarsest spatial resolution data (i.e. EAS and MODIS) showing the least amount of intact forest. For 2000 (Figure 5b), between ESA and MODIS there are considerable differences in the Volta Grande region (Altamira, Jericoá, Vitória do Xingu) with the forest being classified as transitional and dominant between Altamira and Santarém from the MODIS data whereas from ESA there is a large patch of intact forest in the same region. From the finer spatial resolution maps, the Global Forest Cover shows the largest continuous patches of intact forest in comparison to MapBiomas or Fish + Forest which indicate a higher proportion of 'interior' forest and greater fragmentation of the intact forest class. Interestingly, in 2010 (Figure 5c), the high resolution JAXA dataset (25 m spatial resolution) has similarly large patches of intact forest, similar to the coarse spatial resolution ESA and MODIS data. In contrast, the other 30 m datasets (PRODES, Fish + Forest, MapBiomas, TerraClass) all show a high degree of fragmentation especially west of Sinop and Sorriso but also throughout Mato Grosso. The same pattern is seen for the most recent time period (Figure 5d) with the exception of TanDEM-X which has diagonal striping artifacts throughout the study area resulting in an erroneous FAD classification.

The entropy metrics (Figure 6) illustrate the same general pattern as the FAD (Figure 5) but the differences between datasets are more pronounced. For example, even in the oldest time period (Figure 6a), substantial differences between the three datasets can be seen, especially in the north between Itaituba and Altamira with MapBiomas indicating the greatest amount of fragmentation. For the other two data sets, ESA and Fish + Forest, increased entropy can be seen along the road between Itaituba and Altamira, but the fragmentation does not extend as far into the surrounding forest. For the year 2000 (Figure 6b), very high degrees of fragmentation can be seen from all datasets in Mato Grosso and Goías. The larger number of small forest patches in those states in the Global Forest Cover and MapBiomas datasets indicates the highest amount of fragmentation. For 2010 (Figure 6c), ESA and MapBiomas have the largest number of small dispersed patches of forest in the landscape leading to the most fragmented landscape outside of the main intact forest region. That same pattern can be seen for the most recent time period (Figure 6d) for ESA, MODIS, MapBiomas and TanDEM-X. However, the striping artifacts in TanDEM-X greatly increase the fragmentation in the landscape.

The scatterplot between core and edge area from the MSPA statistics further reveal the differences in the spatial patterns of forest fragments in the study area over time between the various datasets (Figure 7). Overall, an expected negative correlation indicating an increase in edge with decrease in core area can be seen. However, the placement in those two axes of the individual datasets representing the same time periods varies greatly. As an outlier, the TanDEM-X map from 2016 indicates the lowest core area in comparison to the amount of edge. This, however, is likely an artifact due to the striping seen in Figures 5 and 6. JAXA, TerraClass and PRODES show the least amount of attrition in core area over time compared to the other datasets whereas ESA has the least amount of change between the two most recent time periods.

Of the water layers examine here only the EC JRC/Google and HydroSHEDS are explicitly water data rather than water being a land cover class extracted as part of a complete land cover classification (Figure 8). The focus on the Volta Grande indicates that there is a lack of connectivity in the water layer from the ESA data (Figure 8d) in the portion of the river north of Jericoá where it is the most seasonably variable (Figure 8a) and at the junction with the Iriri river. This is expected due to the large pixel size of the ESA data in comparison to the relatively narrow channels in this area of the river. Similarly, the JAXA data (Figure 8h) shows discontinuity throughout the river south of Altamira. The TerraClass (Figure 8e) and PRODES (Figure 8j) datasets have the largest extent of surface water, greater than the maximum extent in the EC JRC/Google data (Figure 8b). Oddly, despite the large extent of surface water, both of these datasets lack the Bacajá river (SE tributary of the Xingu) in the Volta Grande (Figure 9) which is present in every other dataset examined here and can be seen in the satellite image from 2017 (Figure 8l).

Because the Belo Monte dam became operational in November 2015 its reservoir should be present in the 2016 through 2018 datasets. In the Landsat image from 2017 (Figure 8l), the flooded channel and reservoir can be clearly seen. Its absence from the TanDEM-X data (Figure 8f) may be explained by the use of the EC JRC/Google surface water layer in the TanDEM-X product (which at the time of writing was only available up to 2015), and the multiple year reference period (2011-2016) over which the radar scenes were gathered. The lack of this large body of water from the PRODES (Figure 8j), MapBiomas (Figure 8i) and TerraClass (Figure 8e) data is more difficult to explain. However, if a pre-existing water layer was used (created prior to the flooding) without explicit classification of water in the more recent imagery, that may account for the lack of the flooded area caused by the Belo Monte dam.

A large difference between mapped surface water and modelled river can be seen with the HydroSHEDS dataset (Figure 8k). The modelled location of water in this area does not always correspond to the actual surface water. Similar to the findings of da Costa et al. (2019), here in the Volta Grande where the river is shallow, braided and traverses relatively flat terrain the course of the river from a DEM derived source greatly differs from datasets where the surface water is directly observed demonstrating a point of failure in this type of terrain for DEM based surface water models.

Discussion

Overall our findings demonstrate the importance of transparency in the generation of remotely sensed datasets. While it is the producers' responsibility to document not only the accuracy of a given classification but also the input sources and methodology used (e.g. inclusion of reference data sets, resolution, validation data source, etc.), it is the user's responsibility to familiarize themselves with the characteristics and limitations of each data set they choose. Apart from obvious differences in granularity (i.e. spatial detail afforded by the different pixel sizes) and data quality (i.e. cloud cover, striping artifacts) the primary reason for the large differences in forest cover between the datasets examined here is not a failure of the technology, rather a difference in the interpretation of 'forest'. Differences in semantics over the meaning of the word have been recorded even in medieval times, with over 800 definitions existing today (Sexton et al. 2016). Internationally for example, FAO uses > 10% tree cover while the International Geosphere-Biosphere Program uses > 60%. Individual countries, programs and agencies typically use a definition somewhere in between.

Our results showcase the importance of further considering the spatial arrangement of forest, not only the overall area covered. As shown in the fragmentation analyses maps may have

similar trends but the total areas of forest and the spatial arrangement of the patches in the landscape may change the outcome of conservation decisions depending on the forest cover map chosen. Users need to take into consideration the appropriateness of the map for their proposed application, not only the popularity of a given dataset.

Despite its importance to all ecosystems and humanity, only ~2.5% of the Earth's water is freshwater and much of it stored in aquifers, glaciers and permanent snow cover (Stiassny 1996). Unsustainable usage is not only affecting the human population and global food security but also the aquatic biota that depend upon those resources (Castello et al. 2013; Frederico et al. 2016). To compound the problem, terrestrial LUCC has a direct and grave impact on the aquatic ecosystems. But herein lies the problem: with few exceptions (e.g. Pekel et al. 2016), surface water is not the main focus in most global/regional/national classifications. And, unfortunately, the dedicated surface water classifications are already out of date. With an upper limit of 2015 for the EC JRC/Google classification for example (at the time of writing), large LUCC projects such as the Belo Monte dam are not included. Users aware of the particular timeline of this hydroelectric project would know that the EC JRC/Google global surface water dataset is not appropriate for conservation questions past 2015 until the dataset becomes updated with more recent imagery and the inclusion of outdated data into more recent land cover classifications (e.g. MapBiomas, TanDEM-X) can have grave ramifications. Similarly, basing conservation decisions on a modelled river network (e.g. HydroSHEDS) without first comparing the network to observed surface water may lead to incorrect assumptions about the ecosystems.

In its inorganic form, mercury is naturally found in Amazonian soils. However, modifications in Amazonian freshwater environments promote chemical reactions that result in its conversion to methylmercury (MeHg), the most toxic form of this metal (Fearnside 2016b;

Nevado et al. 2010). Large construction projects, such as the Belo Monte dam, result in the decomposition of flooded terrestrial vegetation that deteriorates water quality and increases its bioavailability (Hsu-Kim et al. 2018). Former terrestrial islands in the segment of the river between Altamira and Pimental can be seen submerged following the flooding of the reservoir (Figure 10). Given the gravity of the impacts of such large construction projects on entire regions, users must be careful in choosing the most appropriate datasets that accurately take into account the footprint of such projects.

As all datasets here demonstrate, the proliferation of large-scale LUCC in the Xingu basin has continued since the 1980s, the urban centres (e.g. Altamira, Sao Felix do Xingu) have grown, but in parallel, the livelihoods of the population residing outside these primary centres have also undergone changes. These changes are a result of an improved accessibility to markets, for example. And, large scale expansion of the agriculture, energy, mining and forestry sectors within the country. The importance of carefully considering baseline datasets which are accurate spatial representations of the landscape is also key for terrestrial diversity. For example, forest patch connectivity and size of the connecting patches are key factors in the conservation of diversity (Evju and Sverdrup-Thygeson 2016; Parker and Mac Nally 2002; Sauder and Rachlow 2014; Taniguchi et al. 2003).

It is recognized that new Brazilian government policies are a threat to conserving ecosystems across the country (Fearnside 2016a; Fernandes et al. 2017; Freitas et al. 2018; Tollefson 2018). The recent announcement of the administration discrediting INPE's national monitoring programs of the use of remote sensing to quantify forest loss in the Amazon is alarming (Escobar 2019). Our study shows that regardless of the variations in forest cover, all

datasets concur that deforestation is still an issue in Brazil and more needs to be done to protect unique ecosystems like the Xingu river basin.

Acknowledgements

This work was funded by the Natural Sciences and Engineering Research Council of Canada (NSERC) Discovery Grant Program to Kalacska and CNPq #486376/2013-3 and 309815/2017-7 to Sousa. We thank Márcio Vieira, Damilton Rodrigues de Costa (Dani) and Antônio Silva de Oliveira (Toninho) for their help in the field.

Literature Cited

Abell, R., Thieme, M., Ricketts, T.H., et al. 2011. Concordance of freshwater and terrestrial biodiversity. Conservation Letters 4: 127-136.

Abell, R., Thieme, M.L., Revenga, C., et al. 2008. Freshwater ecoregions of the world: A new map of biogeographic units for freshwater biodiversity conservation. Bioscience 58: 403-414.

Abessa, D., Fama, A., & Buruaem, L. 2019. The systematic dismantling of Brazilian environmental laws risks losses on all fronts. Nature Ecology & Evolution 3: 510-511.

Arino, O., Bicheron, P., Achard, F., et al. 2008. GlobCover the most detailed portrait of Earth. ESA Bulletin 136: 25-31.

Barbosa, T.A.P., Benone, N.L., Begot, T.O.R., et al. 2015. Effect of waterfalls and the flood pulse on the structure of fish assemblages of the middle Xingu River in the eastern Amazon basin. Brazilian Journal of Biology 75: S78-S94.

Barona, E., Ramankutty, N., Hyman, G., et al. 2010. The role of pasture and soybean in deforestation of the Brazilian Amazon. Environmental Research Letters 5: 024002

Beaumont, L.J., Pitman, A., Perkins, S., et al. 2011. Impacts of climate change on the world's most exceptional ecoregions. Proceedings of the National Academy of Sciences of the United States of America 108: 2306-2311.

Bontemps, S., Defourny, P., Radoux, J., et al. 2013. Consistent global land cover maps for climate modelling communities: current achievements of the ESA Land Cover CCI. ESA Living Planet Symposium (pp. 1-6). Endiburgh, UK

Brancalion, P.H.S., Garcia, L.C., Loyola, R., et al. 2016. A critical analysis of the Native Vegetation Protection Law of Brazil (2012): updates and ongoing initiatives. Natureza & Conservacao 14: 1-15.

Camargo, M., Giarrizzo, T., & Isaac, V. 2004. Review of the geographic distribution of fish fauna of the Xingu river basin, Brazil. Ecotropica 10: 123-147.

Castello, L., McGrath, D.G., Hess, L.L., et al. 2013. The vulnerability of Amazon freshwater ecosystems. Conservation Letters 6: 217-229.

Chamon, C.C., & Sousa, L.M. 2017. A new species of the leopard pleco genus *Pseudacanthicus* (Siluriformes: Loricariidae) from the Rio Xingu, Brazil. Journal of Fish Biology 90: 356-369.

Costa, A.M., Rizzotto, M.L.F., & Lobato, L.V.C. 2018. The issue of agrochemicals breaks the limits of the ethics of preservation of health and life. Saúde debate 42: 346-353.

Cramer, C.A., & de Sousa, L.M. 2016. A New Species of Tiger Pleco *Panaqolus* (Siluriformes: Loricariidae) from the Xingu Basin, Brazil. Plos One 11: e0165388

da Costa, R.T., Mazzoli, P., & Bagli, S. 2019. Limitations Posed by Free DEMs in Watershed Studies: The Case of River Tanaro in Italy. Frontiers in Earth Science 7: 15.

Da Silva, F.M.R., Oleinski, R.M., Azevedo, A.E.S., et al. 2018a. Vulnerability associated with "symptoms similar to those of mercury poisoning" in communities from Xingu River, Amazon basin. Environmental Geochemistry and Health 40: 1145-1154.

Da Silva, O.M., Dos Santos, M.A., & Dos Santos, L.S. 2018b. Spatiotemporal patterns of deforestation in response to the building of the Belo Monte hydroelectric plant in the Amazon basin. Interciencia 43: 80-84.

de Almeida, C.A., Coutinho, A.C., Esquerdo, J.C.D., et al. 2016. High spatial resolution land use and land cover mapping of the Brazilian Legal Amazon in 2008 using Landsat-5/TM and MODIS data. Acta Amazonica 46: 291-302.

Defourny, P., Kirches, G., Brockmann, C., et al. 2016. Land Cover CCI Product User Guide V2. http://maps.elie.ucl.ac.be/CCI/viewer/download/ESACCI-LC-PUG-v2.5.pdf

Dias, L.C.P., Macedo, M.N., Costa, M.H., et al. 2015. Effects of land cover change on evapotranspiration and streamflow of small catchments in the Upper Xingu River Basin, Central Brazil. Journal of Hydrology-Regional Studies 4: 108-122.

Dias, L.C.P., Pimenta, F.M., Santos, A.B., et al. 2016. Patterns of land use, extensification, and intensification of Brazilian agriculture. Global Change Biology 22: 2887-2903.

Dimiceli, C., Carroll, M., Sohlberg, R., et al. 2015. MOD44B MODIS/Terra Vegetation Continuous Fields Yearly L3 Global 250m SIN Grid V006 [Data set]. https://lpdaac.usgs.gov/products/mod44bv006/

Dinerstein, E., Vynne, C., Sala, E., et al. 2019. A Global Deal for Nature: Guiding principles, milestones, and targets. Science Advances 5: 17.

Durigan, G., Guerin, N., & da Costa, J. 2013. Ecological restoration of Xingu Basin headwaters: motivations, engagement, challenges and perspectives. Philosophical Transactions of the Royal Society B-Biological Sciences 368: 20120165

Esch, T., Heldens, W., Hirner, A., et al. 2017. Breaking new ground in mapping human settlements from space – The Global Urban Footprint. ISPRS Journal of Photogrammetry and Remote Sensing 134: 30-42.

Escobar, H. 2019. Deforestation in the Amazon is shooting up, but Brazil's president calls the data 'a lie'. Science doi:10.1126/science.aay9103

European Commission Joint Research Center 2003. Global Land Cover 2000 database. https://forobs.jrc.ec.europa.eu/products/glc2000/glc2000.php

Evju, M., & Sverdrup-Thygeson, A. 2016. Spatial configuration matters: a test of the habitat amount hypothesis for plants in calcareous grasslands. Landscape Ecology 31: 1891-1902.

FAO 2016. FAOSTAT Statistical Database. Rome, Italy

Fearnside, P.M. 2001. Soybean cultivation as a threat to the environment in Brazil. Environmental Conservation 28: 23-38.

Fearnside, P.M. 2016a. Brazilian politics threaten environmental policies. Science 353: 746-748.

Fearnside, P.M. 2016b. Greenhouse gas emissions from hydroelectric dams in tropical forests. In J. Lehr, & J. Keeley (Eds.), Alternative Energy and Shale Gas Encyclopedia (pp. 428-438). New York: John Wiley & Sons Publishers

Fernandes, G.W., Vale, M.M., Overbeck, G.E., et al. 2017. Dismantling Brazil's science threatens global biodiversity heritage. Perspectives in Ecology and Conservation 15: 239-243.

Ferreira Marmontel, C.V., Lucas-Borja, M.E., Rodrigues, V.A., et al. 2018. Effects of land use and sampling distance on water quality in tropical headwater springs (Pimenta creek, São Paulo State, Brazil). Science of the Total Environment 622-623: 690-701.

Fitzgerald, D.B., Perez, M.H.S., Sousa, L.M., et al. 2018. Diversity and community structure of rapids-dwelling fishes of the Xingu River: Implications for conservation amid large-scale hydroelectric development. Biological Conservation 222: 104-112.

Foley, J.A., Ramankutty, N., Brauman, K.A., et al. 2011. Solutions for a cultivated planet. Nature 478: 337-342.

Foody, G.M. 2004. Thematic map comparison: Evaluating the statistical significance of differences in classification accuracy. Photogrammetric Engineering and Remote Sensing 70: 627-633.

Foody, G.M. 2006. What is the difference between two maps? A remote senser's view. Journal of Geographical Systems 8: 119-130.

Frederico, R.G., Olden, J.D., & Zuanon, J. 2016. Climate change sensitivity of threatened, and largely unprotected, Amazonian fishes. Aquatic Conservation-Marine and Freshwater Ecosystems 26: 91-102.

Freitas, F.L.M., Sparovek, G., Berndes, G., et al. 2018. Potential increase of legal deforestation in Brazilian Amazon after Forest Act revision. Nature Sustainability 1: 665-670.

Fritz, S., & See, L. 2008. Identifying and quantifying uncertainty and spatial disagreement in the comparison of Global Land Cover for different applications. Global Change Biology 14: 1057-1075.

Fuchs, R., Alexander, P., Brown, C., et al. 2019. Why the US–China trade war spells disaster for the Amazon. Nature 567: 451-454.

Gauthier, C., Lin, Z., Peter, B.G., et al. 2019. Hydroelectric Infrastructure and Potential Groundwater Contamination in the Brazilian Amazon: Altamira and the Belo Monte Dam. Professional Geographer 71: 292-300.

Giarrizzo, T., Oliveira, R.R.D., Andrade, M.C., et al. 2015. Length-weight and length-length relationships for 135 fish species from the Xingu River (Amazon Basin, Brazil). Journal of Applied Ichthyology 31: 415-424.

Gilbert, N. 2009. Forest definition comes under fire. Nature News doi:10.1038/news.2009.842

Godfray, H.C.J., Beddington, J.R., Crute, I.R., et al. 2010. Food Security: The Challenge of Feeding 9 Billion People. Science 327: 812-818.

Goulding, M., Barthem, R., & Ferreira, E. 2003. The Smithsonian Atlas of the Amazon. Washington, DC: The Smithsonian Institution

Hansen, M.C., DeFries, R.S., Townshend, J.R.G., et al. 2003. Global Percent Tree Cover at a Spatial Resolution of 500 Meters: First Results of the MODIS Vegetation Continuous Fields Algorithm. Earth Interactions 7: 10

Hansen, M.C., Egorov, A., Roy, D.P., et al. 2011. Continuous fields of land cover for the conterminous United States using Landsat data: first results from the Web-Enabled Landsat Data (WELD) project. Remote Sensing Letters 2: 279-288.

Hansen, M.C., Potapov, P.V., Moore, R., et al. 2013. High-Resolution Global Maps of 21st-Century Forest Cover Change. Science 342: 850-853.

Hansen, M.C., Stehman, S.V., & Potapov, P.V. 2010. Quantification of global gross forest cover loss. Proceedings of the National Academy of Sciences of the United States of America 107: 8650-8655.

Herold, M., Woodcock, C.E., di Gregorio, A., et al. 2006. A joint initiative for harmonization and validation of land cover datasets. IEEE Transactions on Geoscience and Remote Sensing 44: 1719-1727.

Hsu-Kim, H., Eckley, C.S., Acha, D., et al. 2018. Challenges and opportunities for managing aquatic mercury pollution in altered landscapes. Ambio 47: 141-169.

Ilha, P., Rosso, S., & Schiesari, L. 2019. Effects of deforestation on headwater stream fish assemblages in the Upper Xingu River Basin, Southeastern Amazonia. Neotropical Ichthyology 17: e180099

INPE 2015. Projeto PRODES - Monitoramento da Floresta Amazônica Brasileira por Satélite.

Junk, W., Bayley, P.B., & Sparks, R.E. 1989. The flood pulse concept in river-floodplain systems. In D.P. Dodge (Ed.), Proceedings of the International Large River Symposium (LARS) (pp. 110-127): Canadian Special Publication of Fisheries and Aquatic Sciences

Kalacska, M., Lucanus, O., Sousa, L., et al. 2019a. A new multi-temporal forest cover classification for the Xingu River basin, Brazil. Data 4(3):114

Kalacska, M., Lucanus, O., Sousa, L., et al. 2019b. UAV-Based 3D Point Clouds of Freshwater Fish Habitats, Xingu River Basin, Brazil. Data 4(1):9

Klarenberg, G., Munoz-Carpena, R., Perz, S., et al. 2019. A spatiotemporal natural-human database to evaluate road development impacts in an Amazon trinational frontier. Scientific Data 6: 12.

Lambin, E.F., & Meyfroidt, P. 2011. Global land use change, economic globalization, and the looming land scarcity. Proceedings of the National Academy of Sciences of the United States of America 108: 3465-3472.

Latrubesse, E.M., Arima, E.Y., Dunne, T., et al. 2017. Damming the rivers of the Amazon basin. Nature 546: 363-369.

Lees, A.C., Peres, C.A., Fearnside, P.M., et al. 2016. Hydropower and the future of Amazonian biodiversity. Biodiversity and Conservation 25: 451-466.

Lehner, B., Verdin, K., & Jarvis, A. 2008. New global hydrography derived from spaceborne elevation data. EOS 89: 93-104.

Lessa, A.C.R., dos Santos, M.A., Maddock, J.E.L., et al. 2015. Emissions of greenhouse gases in terrestrial areas pre-existing to hydroelectric plant reservoirs in the Amazon: The case of Belo Monte hydroelectric plant. Renewable & Sustainable Energy Reviews 51: 1728-1736.

Levis, C., Costa, F.R.C., Bongers, F., et al. 2017. Persistent effects of pre-Columbian plant domestication on Amazonian forest composition. Science 355: 925

Li, B.B.V., Hughes, A.C., Jenkins, C.N., et al. 2016. Remotely Sensed Data Informs Red List Evaluations and Conservation Priorities in Southeast Asia. Plos One 11: e0160566

Lombardo, U., Szabo, K., Capriles, J.M., et al. 2013. Early and Middle Holocene Hunter-Gatherer Occupations in Western Amazonia: The Hidden Shell Middens. Plos One 8: e72746

Lujan, N.K., & Conway, K.W. 2015. Life in the Fast Lane: A Review of Rheophily in Freshwater Fishes. In R. Riesch, M. Plath, & M. Tobler (Eds.), Extremophile Fishes (pp. 107-136). Dordrecht: Springer

Macedo, M.N., Coe, M.T., DeFries, R., et al. 2013. Land-use-driven stream warming in southeastern Amazonia. Philosophical Transactions of the Royal Society B-Biological Sciences 368: 20120153

Malhi, Y., Roberts, J.T., Betts, R.A., et al. 2008. Climate change, deforestation, and the fate of the Amazon. Science 319: 169-172.

MAPA 2015. Projeções do Agronegócio Brasil 2014/15 a 2024/25. Projeções a longo Prazo. Brasilia, Brazil

MapBiomas Project. MapBiomas Project - Collection v3.1 of the Annual Land Use Land Cover Maps of Brazil.

Martone, M., Rizzoli, P., Wecklich, C., et al. 2018. The global forest/non-forest map from TanDEM-X interferometric SAR data. Remote Sensing of Environment 205: 352-373.

McCallum, I., Obersteiner, M., Nilsson, S., et al. 2006. A spatial comparison of four satellite derived 1 km global land cover datasets. International Journal of Applied Earth Observation and Geoinformation 8: 246-255.

McGarigal, K., Cushman, S.A., & Ene, E. 2012. FRAGSTATS v4: Spatial Pattern Analysis Program for Categorical and Continuous Maps. Computer software program produced by the authors at the University of Massachusetts, Amherst.

McMichael, C.H., Feeley, K.J., Dick, C.W., et al. 2017. Comment on "Persistent effects of pre-Columbian plant domestication on Amazonian forest composition". Science 358: eaan8347

Mello, K., Valente, R.A., Randhir, T.O., et al. 2018a. Effects of land use and land cover on water quality of low-order streams in Southeastern Brazil: Watershed versus riparian zone. CATENA 167: 130-138.

Mello, K.d., Valente, R.A., Randhir, T.O., et al. 2018b. Impacts of tropical forest cover on water quality in agricultural watersheds in southeastern Brazil. Ecological Indicators 93: 1293-1301.

Nepstad, D., McGrath, D., Stickler, C., et al. 2014. Slowing Amazon deforestation through public policy and interventions in beef and soy supply chains. Science 344: 1118-1123.

Nevado, J.J.B., Martin-Doimeadios, R.C.R., Bernardo, F.J.G., et al. 2010. Mercury in the Tapajos River basin, Brazilian Amazon: A review. Environment International 36: 593-608.

Nogueira, C., Buckup, P.A., Menezes, N.A., et al. 2010. Restricted-Range Fishes and the Conservation of Brazilian Freshwaters. Plos One 5: 10.

O'Connor, B., Secades, C., Penner, J., et al. 2015. Earth observation as a tool for tracking progress towards the Aichi Biodiversity Targets. Remote Sensing in Ecology and Conservation 1: 19-28.

Olson, D.M., & Dinerstein, E. 2002. The Global 200: Priority ecoregions for global conservation. Annals of the Missouri Botanical Garden 89: 199-224.

Paganini, M., Leidner, A.K., Geller, G., et al. 2016. The role of space agencies in remotely sensed essential biodiversity variables. Remote Sensing in Ecology and Conservation 2: 132-140.

Parker, M., & Mac Nally, R. 2002. Habitat loss and the habitat fragmentation threshold: an experimental evaluation of impacts on richness and total abundances using grassland invertebrates. Biological Conservation 105: 217-229.

Pekel, J.F., Cottam, A., Gorelick, N., et al. 2016. High-resolution mapping of global surface water and its long-term changes. Nature 540: 418

Pereira, J.C., & Viola, E. 2019. Catastrophic Climate Risk and Brazilian Amazonian Politics and Policies: A New Research Agenda. Global Environmental Politics 19: 93-103.

Pimm, S.L., Ayres, M., Balmford, A., et al. 2001. Environment - Can we defy nature's end? Science 293: 2207-2208.

Proenca, V., Martin, L.J., Pereira, H.M., et al. 2017. Global biodiversity monitoring: From data sources to Essential Biodiversity Variables. Biological Conservation 213: 256-263.

Rajao, R., & Georgiadou, Y. 2014. Blame Games in the Amazon: Environmental Crises and the Emergence of a Transparency Regime in Brazil. Global Environmental Politics 14: 97.

Rajão, R., Moutinho, P., & Soares, L. 2017. The Rights and Wrongs of Brazil's Forest Monitoring Systems. Conservation Letters 10: 495-496.

Rockstrom, J., Steffen, W., Noone, K., et al. 2009. A safe operating space for humanity. Nature 461: 472-475.

Rodrigues, V., Estrany, J., Ranzini, M., et al. 2018. Effects of land use and seasonality on stream water quality in a small tropical catchment: The headwater of Córrego Água Limpa, São Paulo (Brazil). Science of The Total Environment 622-623: 1553-1561.

Rose, R.A., Byler, D., Eastman, J.R., et al. 2015. Ten ways remote sensing can contribute to conservation. Conservation Biology 29: 350-359.

Sabaj Perez, M. 2015. Where the Xingu Bends and Will Soon Break. American Scientist 103: 395-403.

Sanches, R.A., Rossete, A.N., Rezende, A.C.P., et al. 2012. Subsidies for the wetlands protection of xingu river basin (State of Mato Grosso, Brazil). Revista Arvore 36: 489-498.

Sauder, J.D., & Rachlow, J.L. 2014. Both forest composition and configuration influence landscape-scale habitat selection by fishers (*Pekania pennanti*) in mixed coniferous forests of the Northern Rocky Mountains. Forest Ecology and Management 314: 75-84.

Sawakuchi, A.O., Hartmann, G.A., Sawakuchi, H.O., et al. 2015. The Volta Grande do Xingu: reconstruction of past environments and forecasting of future scenarios of a unique Amazonian fluvial landscape. Scientific Drilling 20: 21-32.

Scarrow, R. 2019. Frontiers and deforestation. Nature Plants 5: 124-124.

Schmink, M., Hoelle, J., Gomes, C.V.A., et al. 2019. From contested to 'green' frontiers in the Amazon? A long-term analysis of São Félix do Xingu, Brazil. Journal of Peasent Studies 46: 377-399.

Schwartzman, S., Boas, A.V., Ono, K.Y., et al. 2013. The natural and social history of the indigenous lands and protected areas corridor of the Xingu River basin. Philosophical Transactions of the Royal Society B-Biological Sciences 368: 12.

Sexton, J.O., Noojipady, P., Song, X.P., et al. 2016. Conservation policy and the measurement of forests. Nature Climate Change 6: 192.

Shimada, M., Itoh, T., Motooka, T., et al. 2014. New global forest/non-forest maps from ALOS PALSAR data (2007-2010). Remote Sensing of Environment 155: 13-31.

Silva, J.D., Rodrigues, C., & Pereira, D.I. 2015. Mapping and Analysis of Geodiversity Indices in the Xingu River Basin, Amazonia, Brazil. Geoheritage 7: 337-350.

Skole, D., & Tucker, C. 1993. Tropical deforestation and habitat fragmentation in the amazon - satellite data from 1978 to 1988. Science 260: 1905-1910.

Soille, P., & Vogt, P. 2009. Morphological segmentation of binary patterns. Pattern Recognition Letters 30: 456-459.

Sousa, L., Chaves, M.S., Akama, A., et al. 2018. *Platydoras Birindellii*, New Species of Striped Raphael Catfish (Siluriformes: Doradidae) from the Xingu Basin, Brazil. Proceedings of the Academy of Natural Sciences of Philadelphia 166: 1-13.

Souza-Cruz-Buenaga, F.V.A., Espig, S.A., Castro, T.L.C., et al. 2019. Environmental impacts of a reduced flow stretch on hydropower plants. Brazilian Journal of Biology 79: 470-487.

Stella, J.C., & Bendix, J. 2019. Chapter 5 - Multiple Stressors in Riparian Ecosystems. In S. Sabater, A. Elosegi, & R. Ludwig (Eds.), Multiple Stressors in River Ecosystems (pp. 81-110): Elsevier

Stiassny, M.L.J. 1996. An overview of freshwater biodiversity: With some lessons from African fishes. Fisheries 21: 7-13.

Taniguchi, H., Nakano, S., & Tokeshi, M. 2003. Influences of habitat complexity on the diversity and abundance of epiphytic invertebrates on plants. Freshwater Biology 48: 718-728.

Tófoli, R.M., Dias, R.M., Zaia Alves, G.H., et al. 2017. Gold at what cost? Another megaproject threatens biodiversity in the Amazon. Perspectives in Ecology and Conservation 15: 129-131.

Tollefson, J. 2018. Brazil's new president adds to global threat to science. Nature 563: 5-6.

Townshend, J.R.G., & Justice, C.O. 1988. Selecting the spatial-resolution of satellite sensors required for global monitoring of land transformations. International Journal of Remote Sensing 9: 187-236.

Tsendbazar, N.E., de Bruin, S., Mora, B., et al. 2016. Comparative assessment of thematic accuracy of GLC maps for specific applications using existing reference data. International Journal of Applied Earth Observation and Geoinformation 44: 124-135.

Varella, H.R., & Ito, P.M.M. 2018. Crenicichla Dandara, New Species: The Black Jacundá from the Rio Xingu (Teleostei: Cichlidae). Proceedings of the Academy of Natural Sciences of Philadelphia 166: 1-13

Villas-Boas, A. 2012. De Olho na Bacia do Xingu. Série Cartô Brasil Socioambeintal, v. 5. Instituto Socioambiental, São Paulo, Brazil

Vogt, P., & Riitters, K. 2017. GuidosToolbox: universal digital image object analysis. European Journal of Remote Sensing 50: 352-361.

Westman, W.E., Strong, L.L., & Wilcox, B.A. 1989. Tropical deforestation and species endangerment: the role of remote sensing. Landscape Ecology 3: 97-109.

Winemiller, K.O., McIntyre, P.B., Castello, L., et al. 2016. Balancing hydropower and biodiversity in the Amazon, Congo, and Mekong. Science 351: 128-129.

Zimbres, B., Machado, R.B., & Peres, C.A. 2018. Anthropogenic drivers of headwater and riparian forest loss and degradation in a highly fragmented southern Amazonian landscape. Land Use Policy 72: 354-363.

Table 1. Summary of land cover products used in the comparisons. MMU is the minimum mapping unit in hectares. *Tree cover threshold of greater or equal to 30% applied. **The observational unit is 81 ha (Defourny et al. 2016). All sensors are "passive sensors" relying on reflected solar radiation with the exception of the two marked with a § which are active sensors (radar). †15 sec resolution at the equator is 463.8 m longitude x 460.7 m latitude. At 10°S it becomes 456.8 m longitude x 460.9 m latitude.

Map	Year(s)	Sensor(s)	Pixel size (m)	MMU (ha)	Classes	Reference
ESA	1992, 2000, 2010, 2015	MERIS FR/RR, AVHRR, SPOT-VG, PROBA-V	300	9**	22 land cover classes	Bontemps et al. (2013)
EC JRC/Google	1984-2015	Landsat TM5, 7 ETM+, OLI 8	30	N/A	Surface water occurrence, maximum extent	Pekel et al. (2016)
Fish + Forest	1989, 2000, 2010, 2018	Landsat TM5, OLI 8	30	0.8	Forest, Non-forest, Water	Kalacska et al. (2019a)
Global Forest Change*	2000	Landsat 7 ETM+	30	N/A	percent tree cover	Hansen et al. (2013)
JAXA	2010, 2017	PALSAR§/PALSAR-2§	25	0.5	Forest, Non-forest, Water	Shimada et al. (2014)
HydroSHEDS	2000	Shuttle Radar Topography Mission (SRTM)	15 sec†	N/A	Water	Lehner et al. (2008)
MapBiomas	1989, 2000, 2010, 2017	Landsat TM5, 7 ETM+, OLI 8	30	0.5	27 Land cover classes	http://mapbiomas.org
MODIS Vegetation Continuous Fields *	2000, 2010, 2015	MODIS	250	N/A	percent tree cover	Dimiceli et al. (2015)
PRODES	2010, 2017	Landsat, Terra, CBERS, ResourceSat	90, 30	6.25	5 land cover classes and 19 years of deforestation	INPE (2015); Rajão et al. (2017)

TanDEM-X Global Forest/Non-Forest	2016	TanDEM-X[§]	50	0.5	Forest, non-forest, water	Esch et al. (2017); Martone et al. (2018)
Terra Class Amazônia and Cerrado	2010, 2014	Landsat, MODIS, SPOT-5	30	6.25	15-16 land cover classes	de Almeida et al. (2016); Rajão et al. (2017)

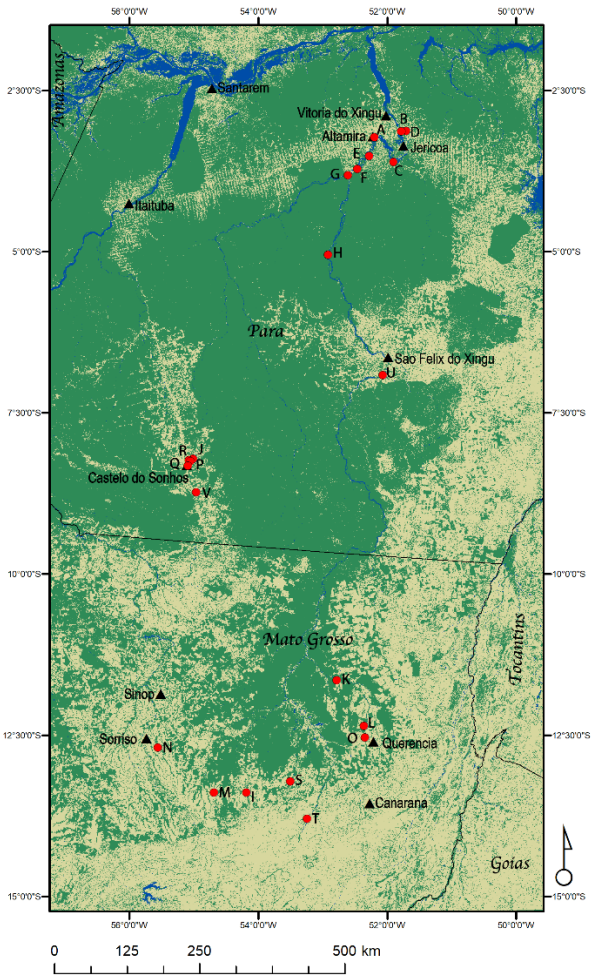

Figure 1. Map of study area with examples of natural and altered land covers. Background map is the forest cover layer from the Fish + Forest 2018 classification (Kalacska et al. 2019a) A) clearing and burning of Arapujá island across from Altamira, B) Belo Monte dam, C) gold mining settlement, D) urban area at the ferry crossing between Belo Monte I and Belo Monte II, E) forest clearing for pasture, F) small homestead, G) confluence of the Xingu and Iriri rivers in the dry season with substrate exposed, H) intact forest in protected area, I) new road construction, J) large scale burning, K) intact forest surrounded by agricultural fields, L) agricultural encroachment on wetlands, M) mega scale cotton plantation, N) irrigated agriculture, O) Riparian forest and wetland surrounded by agriculture, P) illegal mining, Q) urban area, R) forest burning and influx of water contaminated by mine tailings, S) Riparian forest, T) deciduous forest surrounding Culuene rapids, U) large scale forest burning, V) intact forest surrounding Curuá rapids with the Hydro Energia Buriti dam reservoir in the background. 3D reconstructions of the landscape shown in T and V are available from (Kalacska et al. 2019b). Photographs taken by the authors.

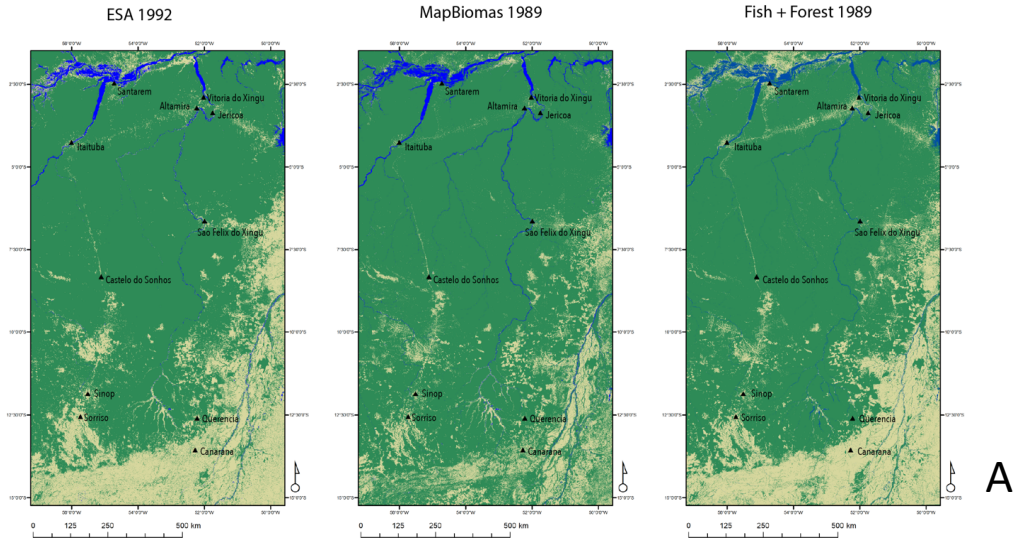

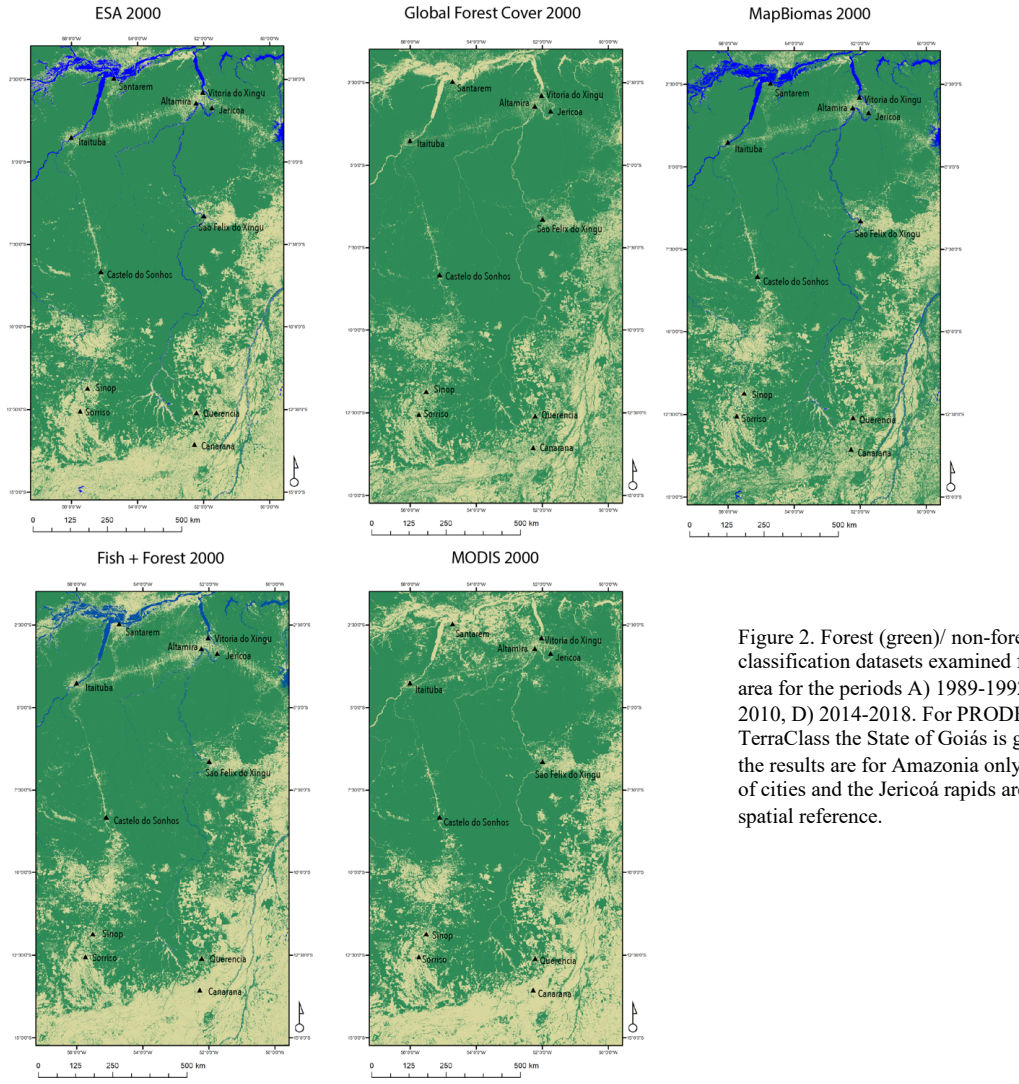

Figure 2. Forest (green)/ non-forest classification datasets examined for the study area for the periods A) 1989-1992, B) 2000, C) 2010, D) 2014-2018. For PRODES and TerraClass the State of Goiás is greyed out as the results are for Amazonia only. Locations of cities and the Jericoá rapids are shown for spatial reference.


ESA 2010
JAXA 2010
MapBiomas 2010
Fish + Forest 2010
MODIS 2010
PRODES 2010
TerraClass 2010
C
ESA 2015
JAXA 2017
MapBiomas 2017
Fish + Forest 2018
MODIS 2015
PRODES 2017
TerraClass 2014
TanDEM-X 2016
D
Santarem
Vitoria do Xingu
Altamira
Jericoa
Itaituba
São Felix do Xingu
Castelo do Sonhos
Sinop
Sorriso
Querencia
Canarana
0 125 250 500 km

Figure 2

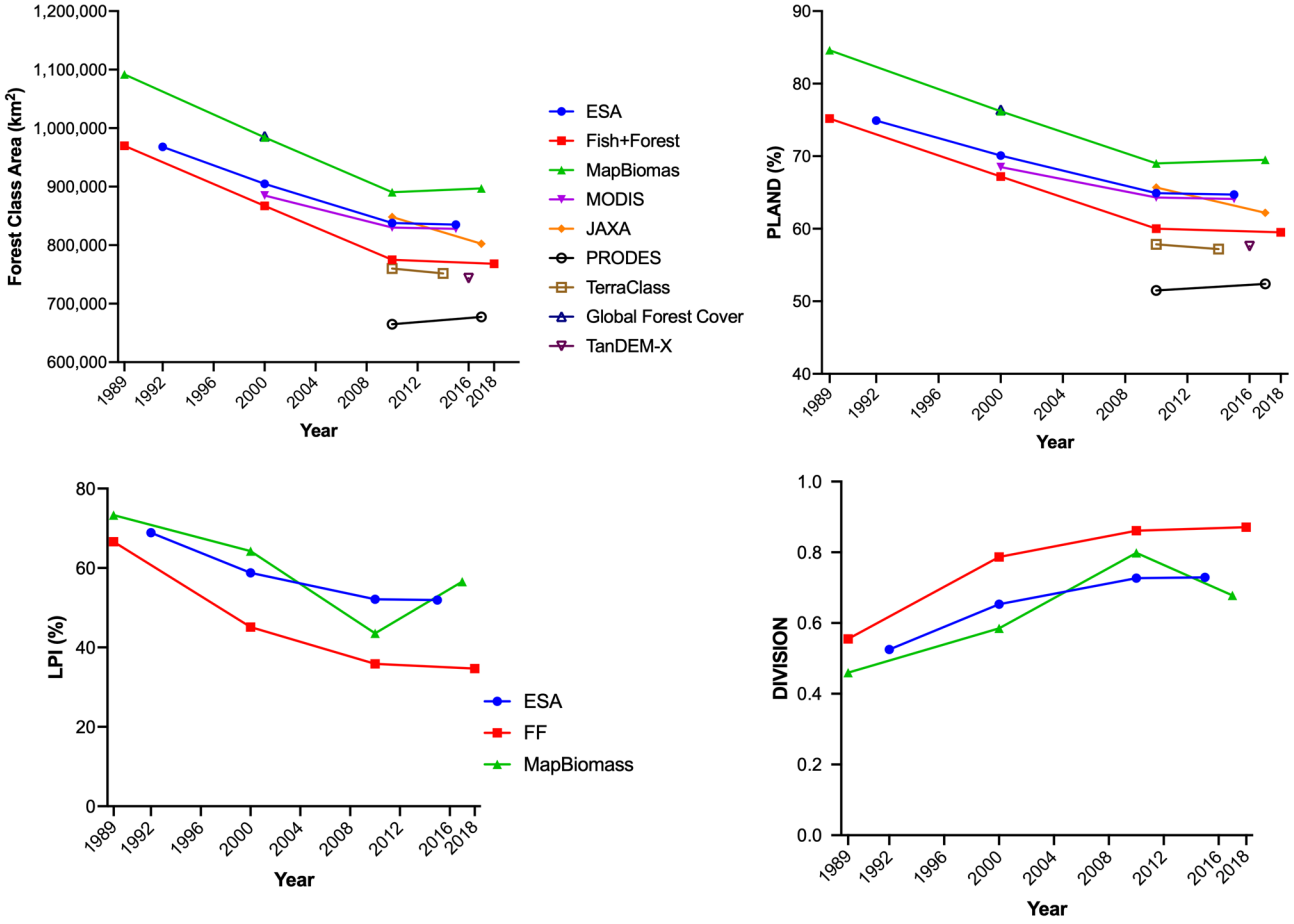

Figure 3. Comparison of total forest area change and fragmentation metrics for the land cover classifications. A) Total forest area (km²), B) PLAND, C) LPI, D) DIVISION. Metrics of PLAND, LPI and DIVISION are only shown for the datasets for all four time periods.

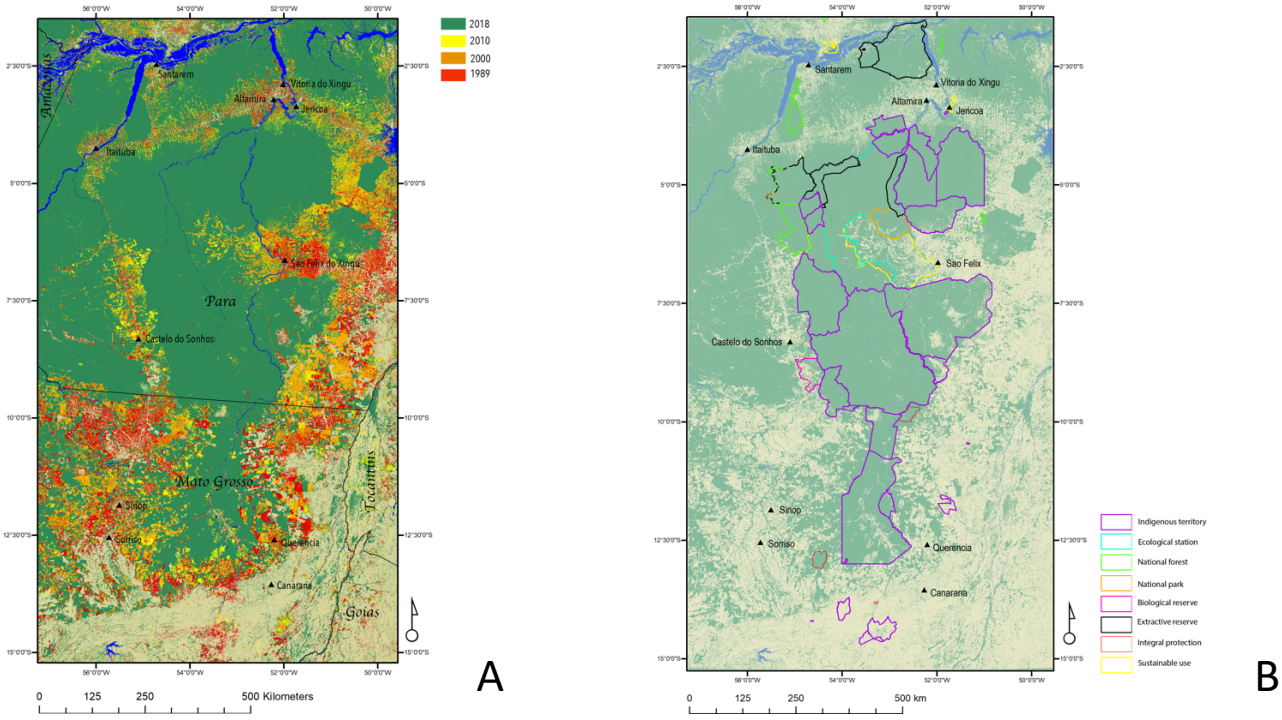

Figure 4 A) change in forest cover extent from 1989 – 2018 from the Fish + Forest classifications. B) Locations of federal and state protected areas and indigenous territories. Background map is the 2018 Fish + Forest classification.

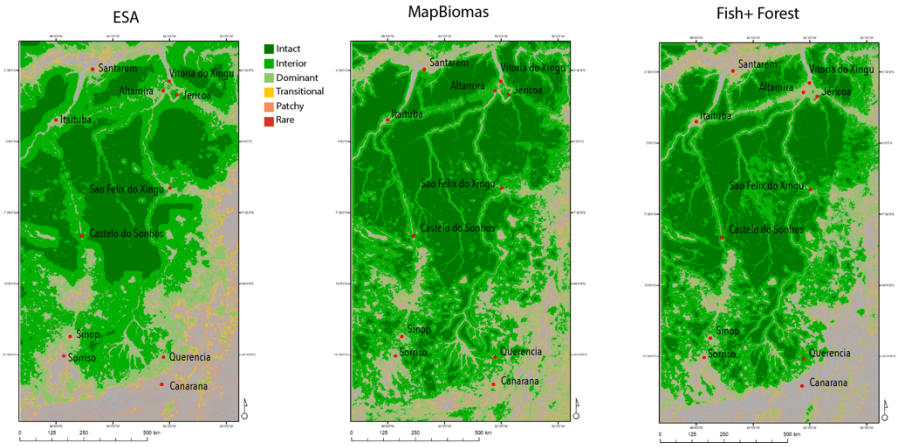

A

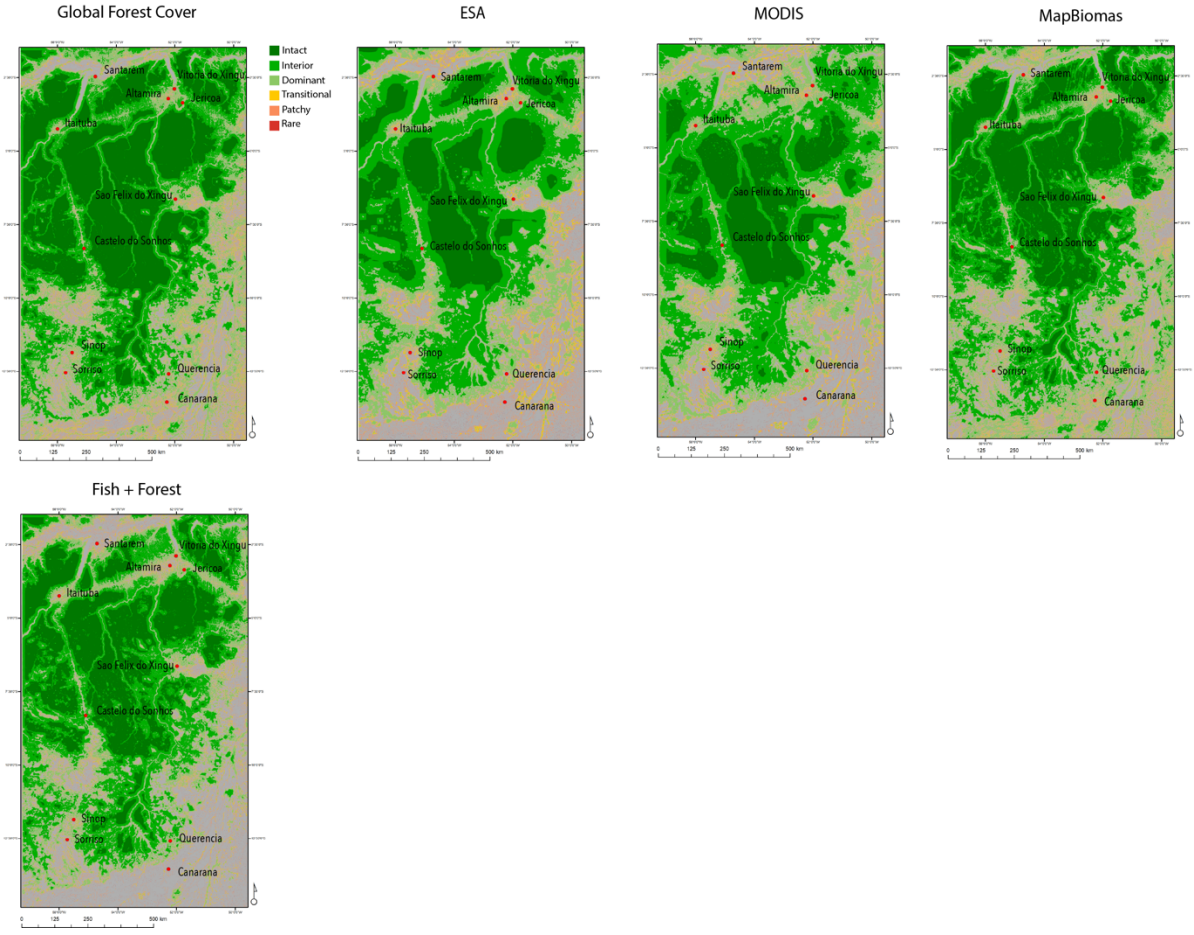

B

Figure 5. Average Foreground Area Density (FAD) classes for the A) 1989-1992, B) 2000, C) 2010, D) 2014-2018 time periods.

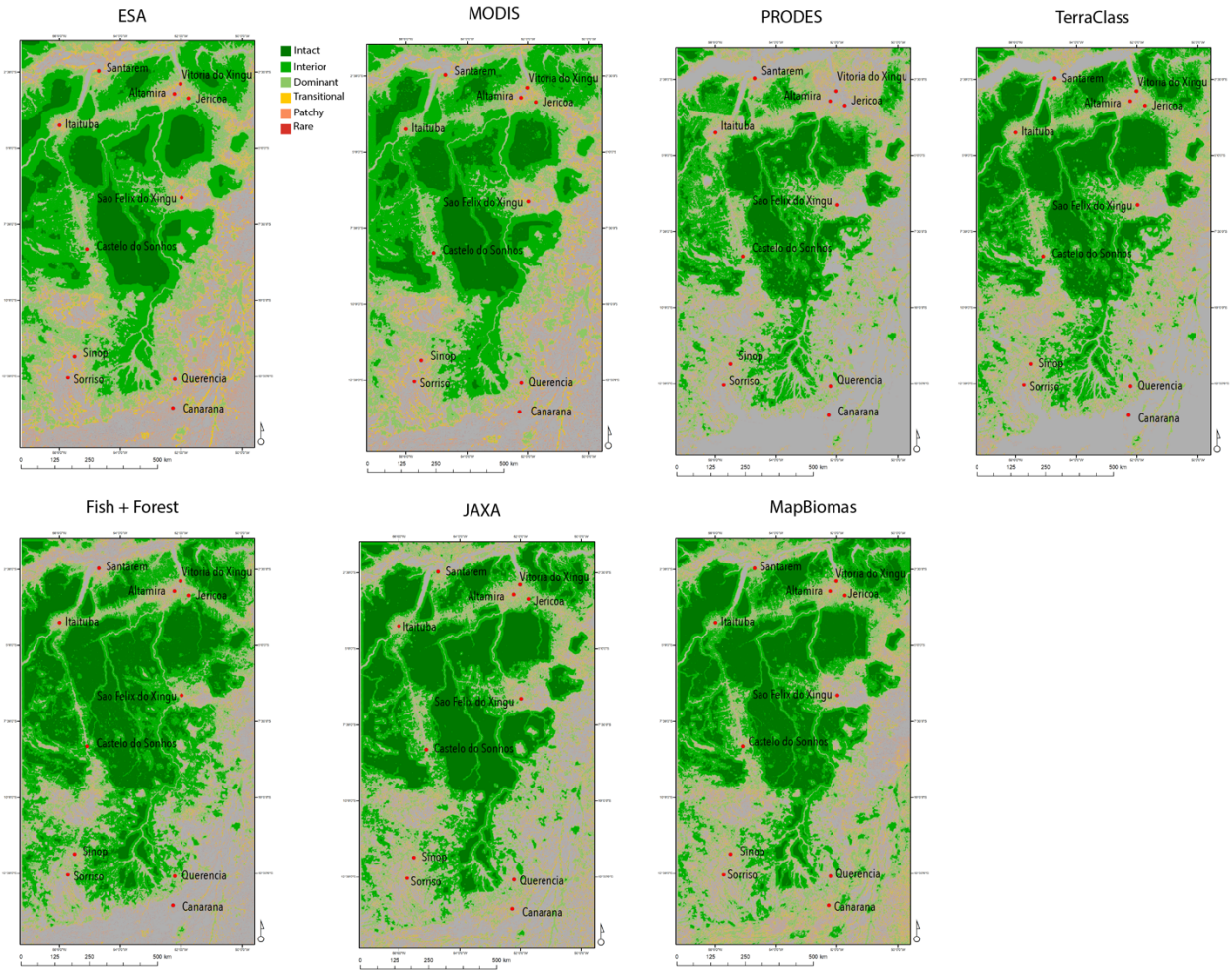
ESA
MODIS
PRODES
TerraClass
Fish + Forest
JAXA
MapBiomas
Intact
Interior
Dominant
Transitional
Patchy
Rare
Santarem
Vitoria do Xingu
Altamira
Jericoa
Itaituba
Sao Felix do Xingu
Castelo do Sonhos
Sinop
Sorriso
Querencia
Canarana
0
125
250
500 km

C

Figure 5.

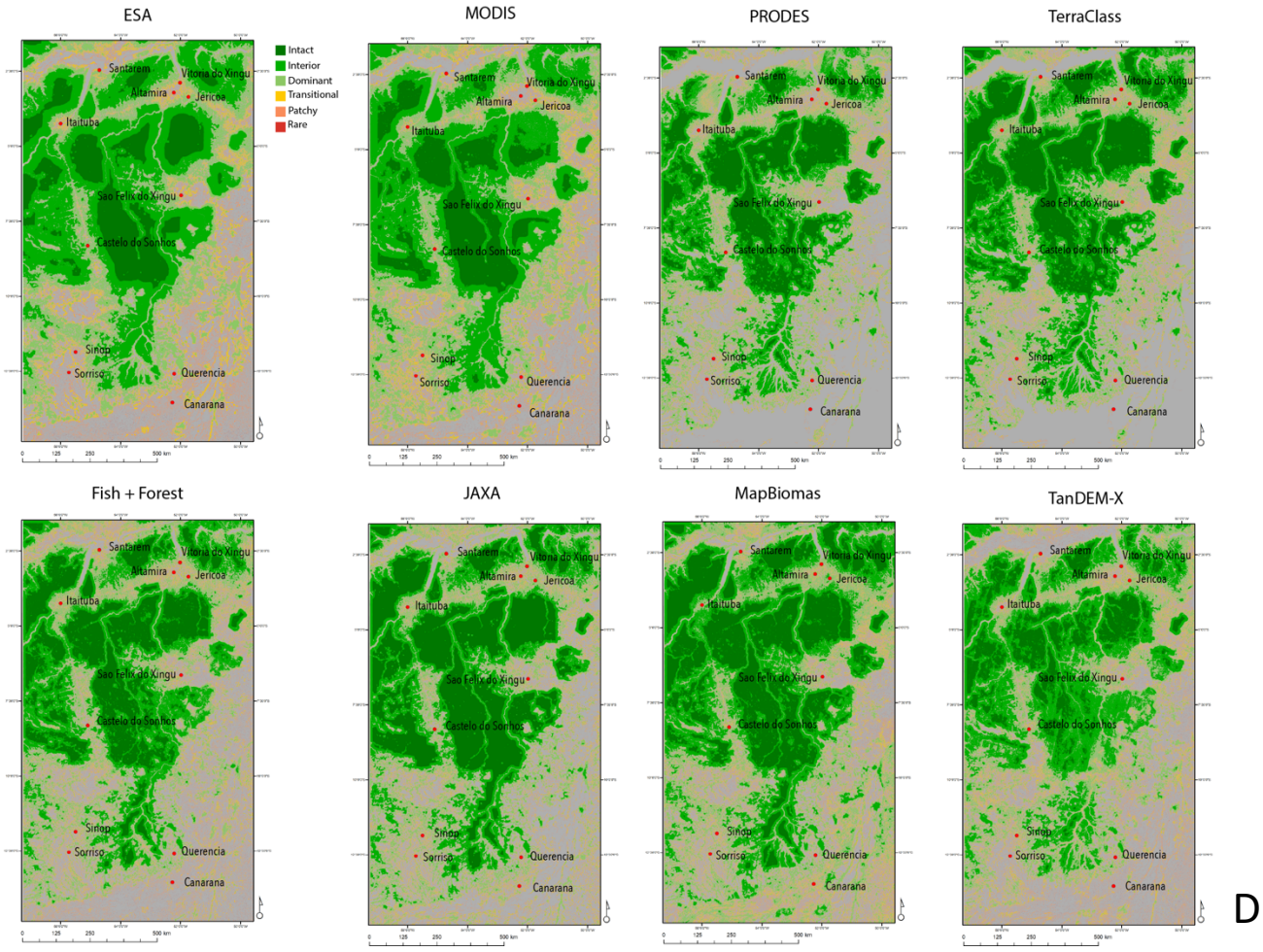
ESA
MODIS
PRODES
TerraClass
Fish + Forest
JAXA
MapBiomas
TanDEM-X
Intact
Interior
Dominant
Transitional
Patchy
Rare
Santarem
Vitoria do Xingu
Altamira
Jericoa
Itaituba
Sao Felix do Xingu
Castelo do Sonhos
Sinop
Sorriso
Querencia
Canarana
D

Figure 5

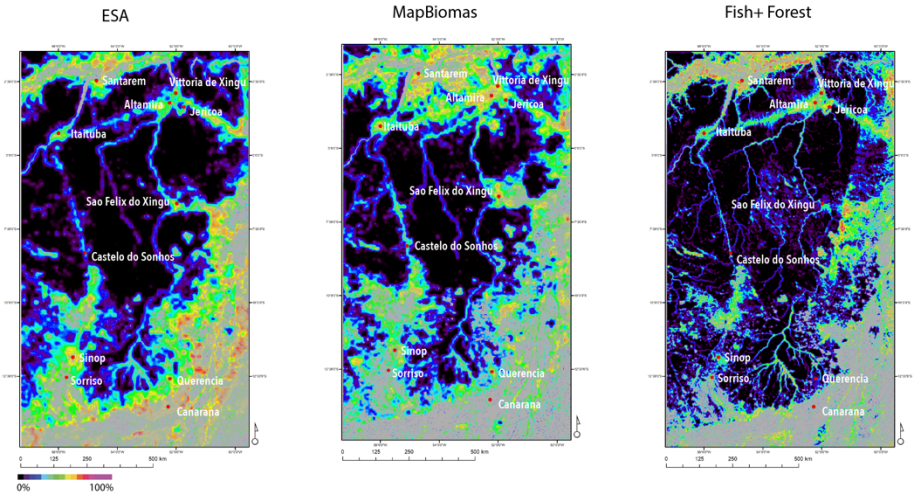

A

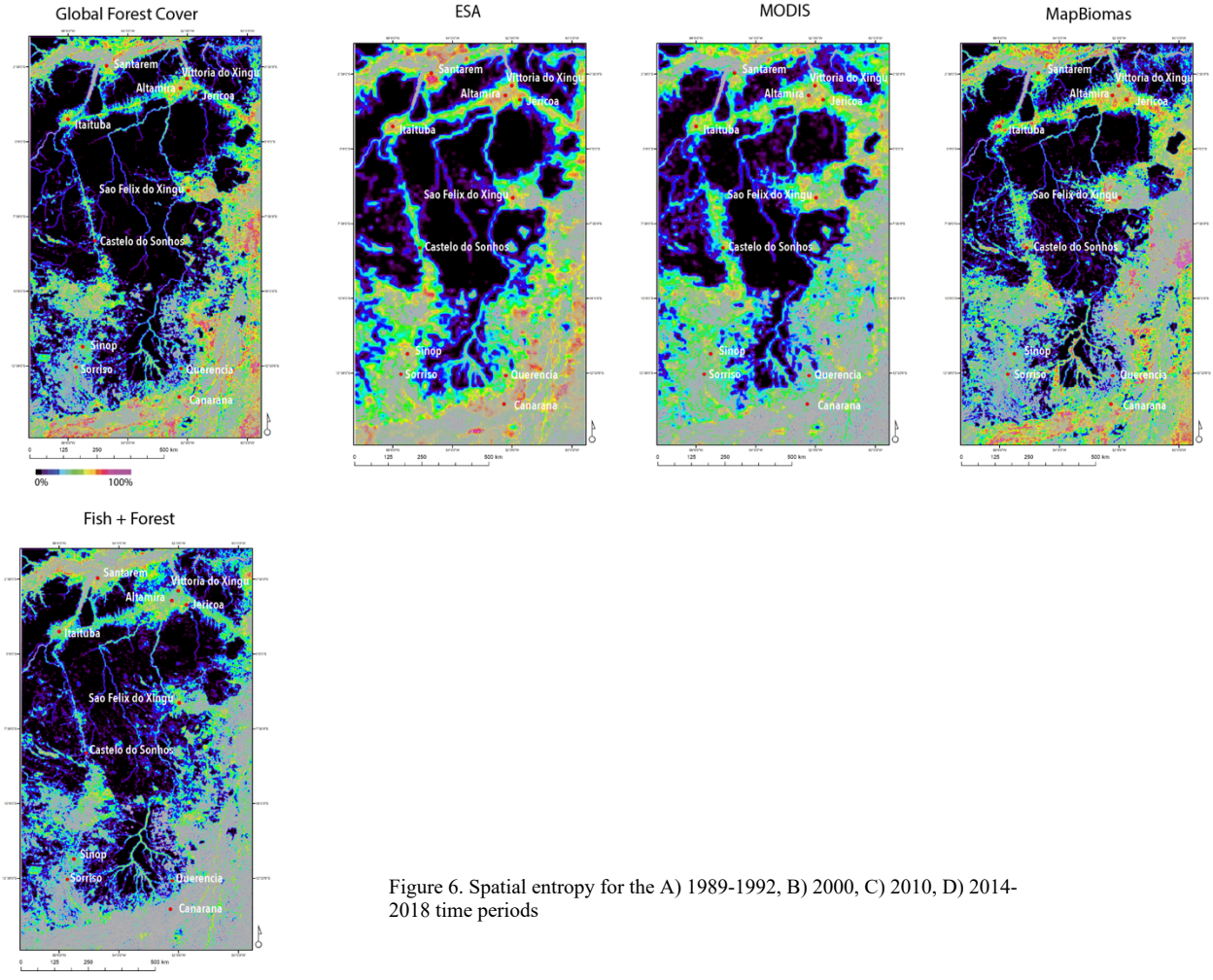

Figure 6. Spatial entropy for the A) 1989-1992, B) 2000, C) 2010, D) 2014-2018 time periods

B

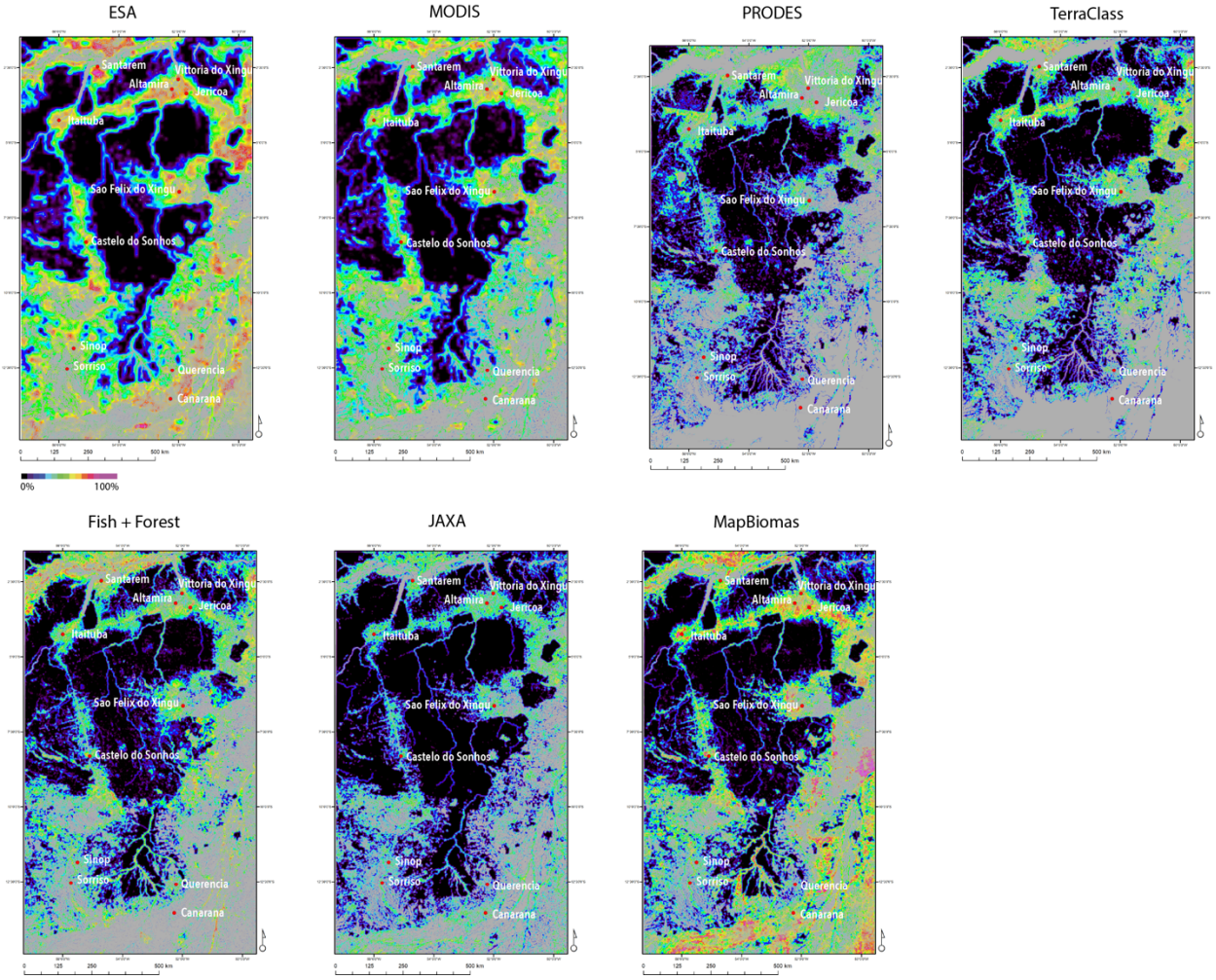
ESA
MODIS
PRODES
TerraClass
Fish + Forest
JAXA
MapBiomas
Santarem
Vittoria do Xingu
Altamira
Jericoa
Itaituba
Sao Felix do Xingu
Castelo do Sonhos
Sinop
Sorriso
Querencia
Canarana
0%
100%
0
125
250
500 km

C

Figure 6.

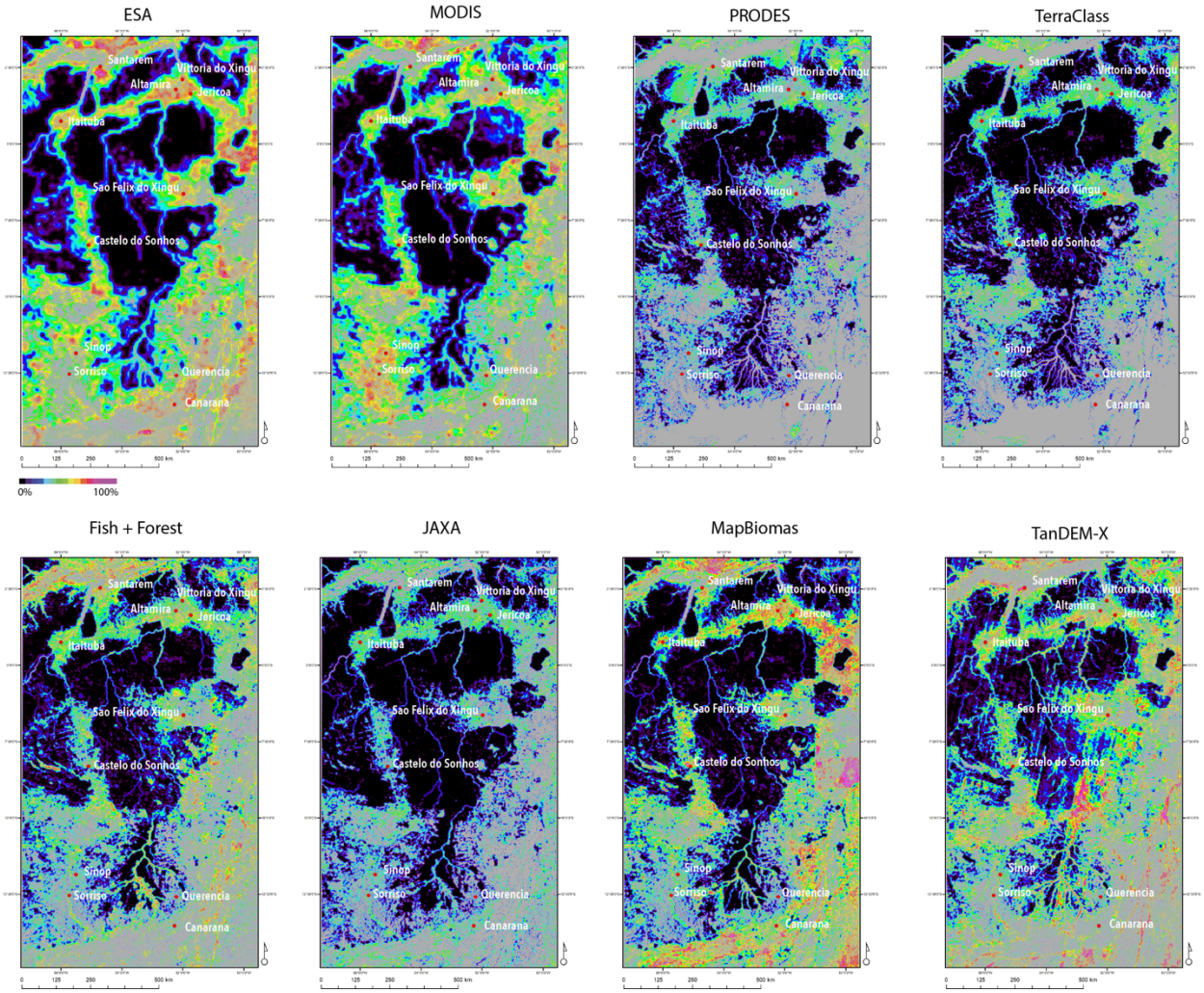
ESA
MODIS
PRODES
TerraClass
Fish + Forest
JAXA
MapBiomas
TanDEM-X
Santarem
Vittoria do Xingu
Altamira
Jericoa
Itaituba
Sao Felix do Xingu
Castelo do Sonhos
Sinop
Sorriso
Querencia
Canarana
0%
100%
0
125
250
500 km

D

Figure 6

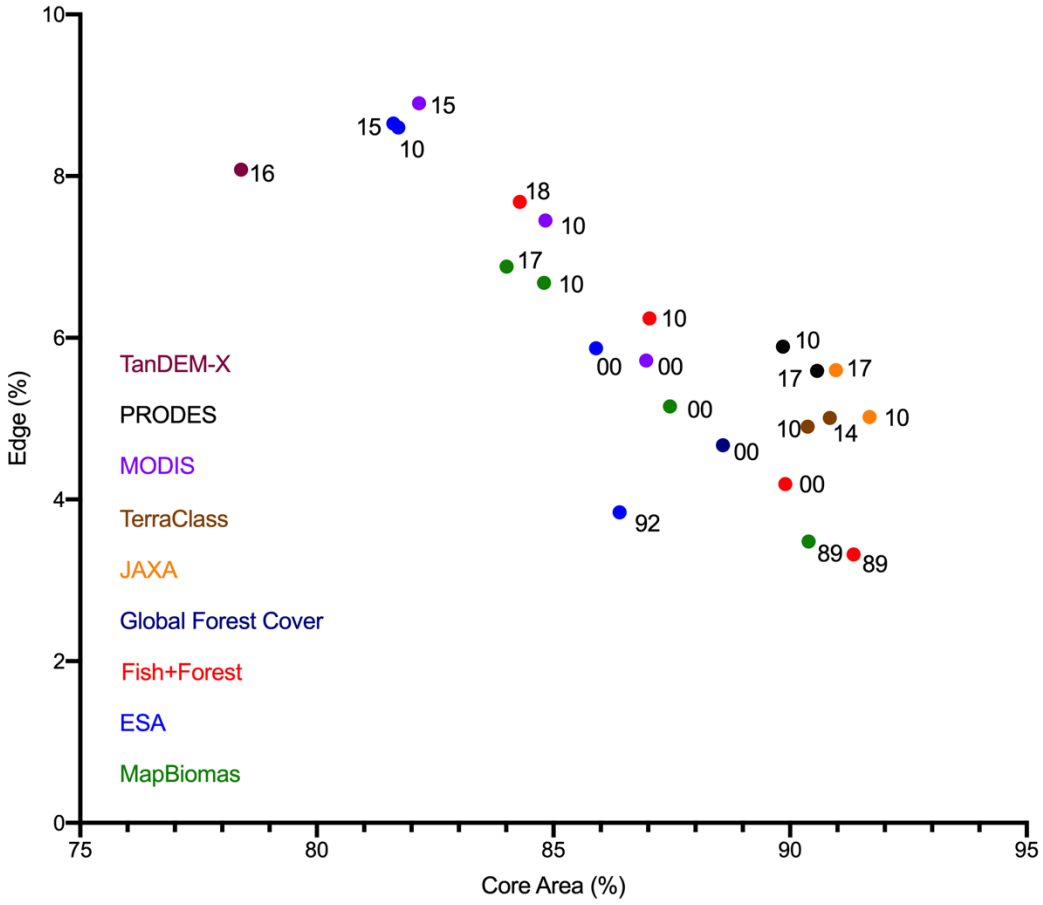

Figure 7. Relationship between MSPA statistics ‘core area’ and ‘edge’ for the forest class from the different datasets. The numbers represent the year of the classification.

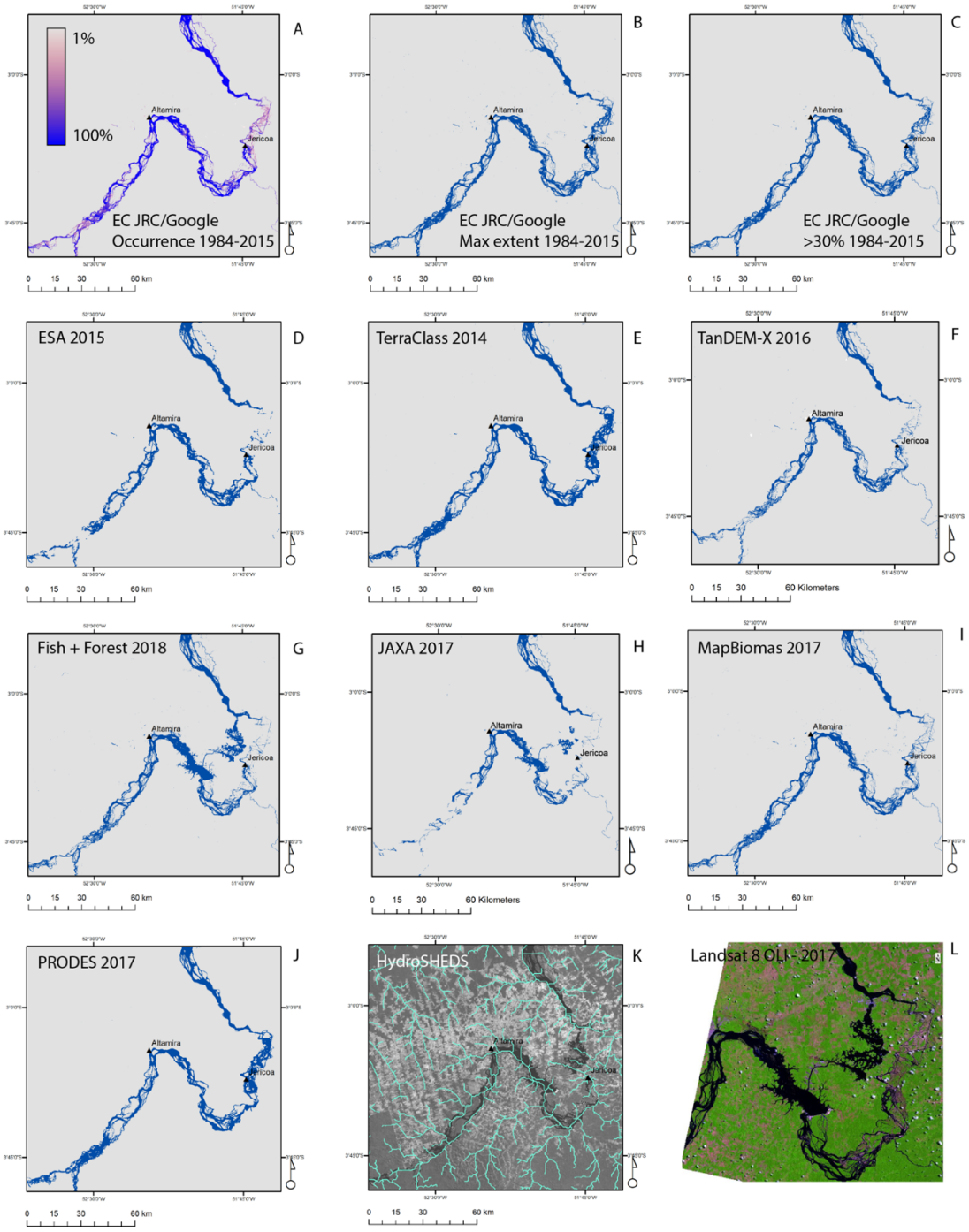

Figure 8. Examples of surface water classifications. Volta Grande area is shown in detail. A) Probability of surface water occurrence over the 1984-2015 period (EC JRC/Google), B) maximum extent over the 1984-2015 period (EC JRC/Google), C) probability of occurrence greater than 30% over the 1984 – 2015 period (EC JRC/Google), D) ESA 2015, E) TerraClass 2014, F) TanDEM-X 2011-2016 period, G) Fish + Forest 2018, H) JAXA 2017, I) MapBiomas 2017, J) PRODES 2017, K) HydroSHEDS overlain on a single band from a Landsat OLI 8 image from 2017 for context, L) Landsat 8 OLI image acquired in 2017 illustrating the Belo Monte reservoir and the dewatered section of the Volta Grande near Jericoá.

Figure 9. Photograph of the Bacajá river taken at its confluence with the Xingu river in the dry season. As a larger tributary of the Xingu river it should be present in hydrographic layers. (Photograph by O. Lucanus)

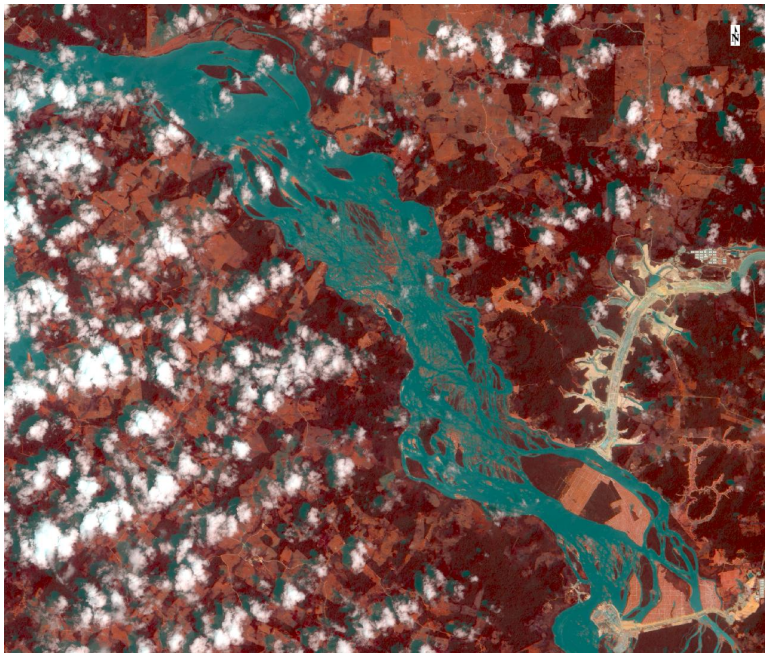

A

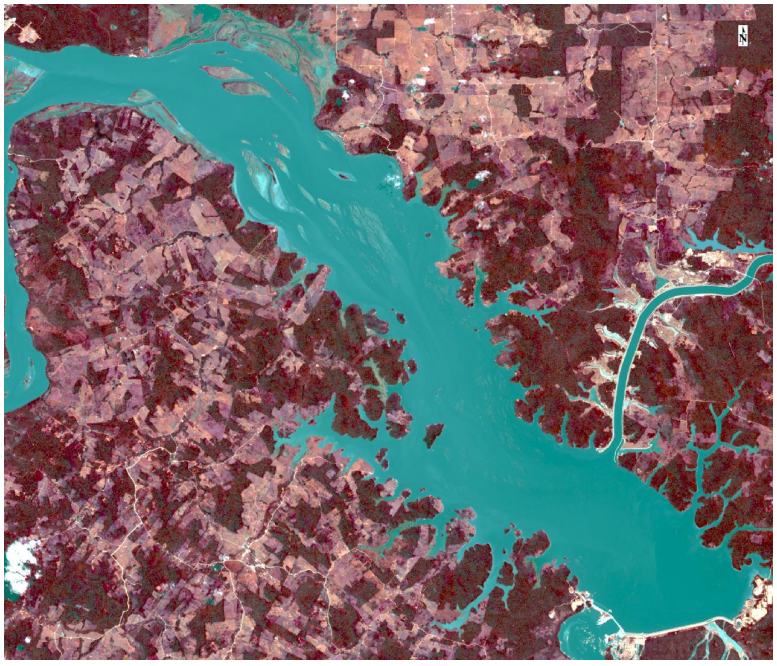

B

Figure 10. A) Landsat 8 OLI image from November 1, 2014; B) Landsat 8 OLI image from July 26, 2019; The satellite images in A and B are shown as a shortwave infrared (R):red (G): blue (B) color composite. C) Original course of the river from (a) shown in blue superimposed on the surface water from (b). The flooding in the reservoir and channel following operationalization of Belo Monte can be clearly seen.

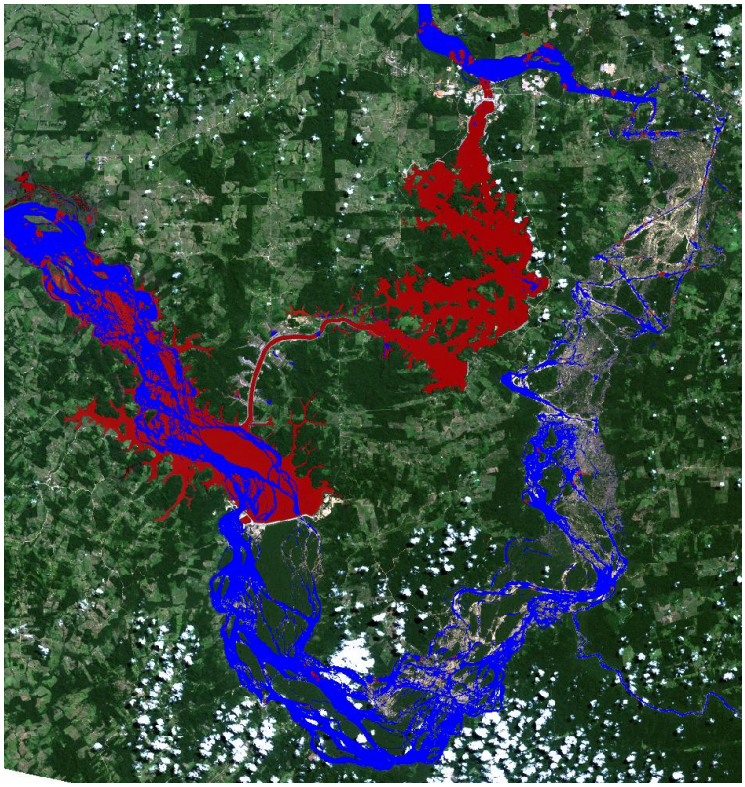

C

Figure 10